AWARD NUMBER: W81XWH-14-1-0297

TITLE: Small Molecule Protection of Bone Marrow Hematopoietic Stem Cells

PRINCIPAL INVESTIGATOR: Raymond J. Monnat, Jr. M.D.

CONTRACTING ORGANIZATION: University of Washington
Seattle WA 98195

REPORT DATE: December 2017

TYPE OF REPORT: Final

PREPARED FOR: U.S. Army Medical Research and Materiel Command
Fort Detrick, Maryland 21702-5012

REPORT DOCUMENTATION PAGE

Form Approved
OMB No. 0704-0188

1. REPORT DATE Dec 2017

2. REPORT TYPE Final

3. DATES COVERED
30 Sep 2014 - 29 Sep 2017

4. TITLE AND SUBTITLE
'Small Molecule Protection of Bone Marrow Hematopoietic Stem Cells'

5a. CONTRACT NUMBER

5b. GRANT NUMBER
W81XWH-14-1-0297

5c. PROGRAM ELEMENT NUMBER

6. AUTHOR(S)
Raymond J. Monnat, Jr. M.D. P.I.
Departments of Pathology and Genome Sciences
University of Washington, Seattle WA 98195
E-Mail: monnat@u.washington.edu

5d. PROJECT NUMBER

5e. TASK NUMBER

5f. WORK UNIT NUMBER

7. PERFORMING ORGANIZATION NAME(S) AND ADDRESS(ES)
University of Washington
4333 Brooklyn Avenue NE
Seattle. WA 98195-0001

8. PERFORMING ORGANIZATION REPORT NUMBER

9. SPONSORING / MONITORING AGENCY NAME(S) AND ADDRESS(ES)
U.S. Army Medical Research and Materiel Command
Fort Detrick, Maryland 21702-5012

10. SPONSOR/MONITOR'S ACRONYM(S)

11. SPONSOR/MONITOR'S REPORT NUMBER(S)

12. DISTRIBUTION / AVAILABILITY STATEMENT
Approved for Public Release; Distribution Unlimited

13. SUPPLEMENTARY NOTES

14. ABSTRACT
During the above project period we:
1. demonstrated the ability of two small molecules, metformin and aminoguanidine, to improve growth, suppress aldehyde-induced DNA damage, and improve aldehyde dose-dependent survival of FANCG-deficient human cells.
2. used of a combination of chemical determination and dose-response assays to provide mechanistic insight into likely mechanisms by which each small molecule provides aldehyde dose-dependent protection in human cells.
3. developed a new quantitative formaldehyde-DNA adduct/crosslink HPLC-MS/MS assay.
4. small molecule suppression of markers of DNA damage in human cells in culture, and improved hematopoiesis and delayed cancer formation in a metformin-treated murine model of Fanconi anemia.
5. completed and published two manuscripts related to this work.

15. SUBJECT TERMS
CD34+ human hematopoietic stem cells (HSCs), bone marrow, formaldehyde toxicity

16. SECURITY CLASSIFICATION OF:			**17. LIMITATION OF ABSTRACT**	**18. NUMBER OF PAGES**	**19a. NAME OF RESPONSIBLE PERSON**
a. REPORT	**b. ABSTRACT**	**c. THIS PAGE**			USAMRMC
Unclassified	Unclassified	Unclassified	Unclassified	34	**19b. TELEPHONE NUMBER** *(include area code)*

Standard Form 298 (Rev. 8-98)
Prescribed by ANSI Std. Z39.18

Table of Contents

Page(s)

1. **Introduction……** 3
2. **Keywords……** 3
3. **Accomplishments……..……...** 3
4. **Impact……...……** 10
5. **Changes/Problems...…..……** 10
6. **Products……..……..…..……** 10
7. **Participants & Other Collaborating Organizations……** 10
8. **Special Reporting Requirements……** 10
9. **Appendices……** 11

1. INTRODUCTION:

Goal: The goal of the proposed research is to determine whether several recently identified small molecules can protect hematopoietic stem cells (HSCs) from damage or killing by endogenous aldehydes. Proof-of-concept for these experiments has been developed using isogenic (mutant/complemented) human cell line pairs from patients with Fanconi anemia (FA), a heritable human bone marrow failure (BMF) syndrome in which HSCs and other cell types are hypersensitive to selected types of DNA damage. The proposed research addresses a key question—the relationship between DNA damage and cell killing—and may identify small molecules that protect HSCs from an important endogenous source of DNA damage. These small molecules could be therapeutically useful in reducing the risk of BMF in diseases such as Fanconi anemia, and perhaps after radiation exposure. The proposed research thus has the potential to catalyze new basic and translational research focused on achieving the BMFRP goals of understanding and curing BMF diseases.

2. KEYWORDS: Provide a brief list of keywords (limit to 20 words).

Fanconi anemia
bone marrow failure
CD34+ hematopoietic stem cells
aldehydes
formaldehyde
DNA damage
DNA base adduct
DNA-protein crosslink
mass spectrometry

3. ACCOMPLISHMENTS:

Our stated goals and timetable for the scope of work are provided in our Revised Scope of Work Table below.

***Revised* Specific Aim 1: Small molecule protection of human cells from aldehyde-induced killing (*in vitro* studies - no mice or human subjects)**	**Timeline**	**Site(s)**	
Major Task 1: Generate and confirm FANCG protein-depleted human CD34+ cells	**Months**	**Site 1**	**Site 2**
Transduce CD34+ cells with GFP/RFP + *FANCG*-specific shRNA lentiviruses	1 - 9	Dr. Monnat	–
Quantify FANCG protein depletion extent and time course by Western blot analysis	9 - 12	Dr. Monnat	–
Milestone Achieved: FANCG-depleted CD34+ cells	1 - 12	Dr. Monnat	–
Major Task 2: *In vitro* formaldehyde dose and small molecule protection of FANCG-depleted human CD34+ cells			
Determine formaldehyde dose-dependent survival on FANCG-deficient/control CD34+ cells in culture	9 - 15	Dr. Monnat	–

Determine small molecule dose-dependent protection from formaldehyde toxicity/cell killing	12 - 18	Dr. Monnat	–
Milestone(s) Achieved: validation of small molecule formaldehyde antagonism in human CD34+ cells	9 - 18	Dr. Monnat	–
***Revised* Specific Aim 2: Does small molecule formaldehyde damage protection result from a reduction in DNA damage?**			
Major Task 1: Develop/validate stable isotope mass spec assay of formaldehyde DNA damage			
Develop adduct/crosslink assays on new UPLC-MS/MS device	1 - 9	–	Dr. Swenberg
Demonstrate detection of formaldehyde-induced DNA damage using DNA isolated from CD34+ cells	9 - 15	Dr. Monnat	Dr. Swenberg
Milestone(s) Achieved: validated high-sensitivity detection of DNA damage in CD34+ progenitor cells	1 - 15	Dr. Monnat	Dr. Swenberg
Major Task 2: Apply mass spectrometric assay to DNA derived from treated CD34+ cells			
Quantify DNA damage in formaldehyde-treated CD34+ cells using isotope-labeling/MS methods	15-24	Dr. Monnat	Dr. Swenberg
Quantify DNA damage by MS in formaldehyde-treated FANCG-depleted CD34+ cells treated with the most effective small molecule antagonist	18-36	Dr. Monnat	Dr. Swenberg
Milestone(s) Achieved: Test of hypothesis that SM protection from aldehyde damage acts at the level of DNA adduct/damage reduction	15-36	Dr. Monnat	Dr. Swenberg

– What was accomplished under these goals?

During the above project period we:

1. demonstrated the ability of two small molecules, metformin and aminoguanidine, to improve growth, suppress aldehyde-induced DNA damage, and improve aldehyde dose-dependent survival of FANCG-deficient human cells.
2. used of a combination of chemical determination and dose-response assays to provide mechanistic insight into likely mechanisms by which each small molecule provides aldehyde dose-dependent protection in human cells.
3. developed a new quantitative formaldehyde-DNA adduct/crosslink HPLC-MS/MS assay.
4. demonstrated small molecule suppression of markers of DNA damage in human cells in culture, and improved hematopoiesis and delayed cancer formation in a metformin-treated murine model of Fanconi anemia.
5. completed and published two manuscripts related to this work.

Revised Specific Aim 1:

Major Task 1: Generate and confirm FANCG or FANCA protein-depleted human CD34+ cells

Accomplishments: In the award period we:

- developed Western blot assays to detect and quantify depletion in human cells;

- identified, after extensive search, 2 *FANCG* shRNAs and 3 *FANCA* shRNAs that can substantially and reproducibly deplete FANCG or FANCA protein respectively from human cells (to ≥90% depletion) after 5 days of shRNA expression.
- generated inducible *FANCG* shRNA lentiviral expression vectors to use to transduce and inducibly deplete FANCG protein from human CD34+ cells.
- transduce CD34+ cells with *FANCA* or *FANCG* –specific shRNA lentiviral vectors in order to deplete FANCA and/or FANCG. Due to low transduction efficiency on repeated trials, the number of transduced CD34+ cells were not large enough to feed both cell survival and mass spectrometry assays.

Major Task 2: *In vitro* formaldehyde dose and small molecule protection of FANCG-depleted human CD34+ cells.

Accomplishments: In the award period we:
- demonstrated substantial, reproducible mitotic expansion of human peripheral blood mobilized CD34+ cells in defined media.
- confirmed ability of small molecules to partially suppress differentiation with loss of cell surface antigen staining during CD34+ *in vitro* mitotic expansion.
- determined formaldehyde dose-survival curve using mitotically expanded CD34+ cells.
-demonstrated ability of two small molecule protectants, metformin and aminoguanidine, to improve the growth, suppress aldehyde-induced DNA damage and improve the aldehyde dose-dependent survival of FANCG-deficient human cells.
- used a combination of chemical determination and dose-response assays to provide mechanistic insight into likely mechanisms by which each small molecule provides aldehyde dose-dependent protection in human cells in culture.

Next steps:

This is the final report for this award.

Revised Specific Aim 2: Does small molecule formaldehyde damage protection result from a reduction in DNA damage?

Major Task 1: Develop/validate stable isotope mass spec assay of formaldehyde DNA damage (in conjunction with collaborator James Swenberg/University of North Carolina).

Accomplishments: In the award period we:
- developed and published new quantitative formaldehyde-DNA adduct/crosslink HPLC-MS/MS assays.
- demonstrated application of mass spectrometry-based methods to quantify DNA damage due to formaldehyde in *Adh5(-/-)Fancd2(-/-)* deficient mice and related control genotypes (this work was performed collaboratively and independently of this award by Dr. Swenberg and Dr. KJ Patel at the MRC Lab of Molecular Biology).

Major Task 2: Apply mass spectrometric assay to DNA derived from treated CD34+ cells (in conjunction with collaborator James Swenberg/University of North Carolina).

Next steps:

This is the final report for this award.

The following sections provide additional technical detail and results for each of the above accomplishments.

Aim 1 - Major Task 1: Demonstrate of lentiviral depletion of FANCG proteins from human cells.

Screen to identify shRNAs for human FANCG protein depletion: We screened a large number (>12) of human *FANCG*-specific shRNAs from various sources to identify two that gave consistent, reproducible and substantial (≥90%) depletion of FANCG protein from human cells. Two of these (shFG31 and shFG32, shown below), when transferred to and expressed from a lentiviral vector backbone, again were shown to reproducibly deplete to ≥90% FANCG protein from human cells.

***Western blot verification of FANCG depletion by shRNA*:** Whole cell lysates from GM639 human SV40-transformed fibroblasts (Expt. 1) and U2-OS human osteosarcoma cells (Expt. 2) that were either untransduced (untx), transduced with and expressing a scrambled shRNA (shCTR), or transduced with and expressing one of 4 *FANCG*-targeting shRNAs (shFG31, shFG32, shFG33, and shFG34) were blotted with extracts from a control isogenic human FANCG-deficient/complemented lymphoblastoid cell line pair (EUFA316, negative control for FANCG protein expression) and its FANCG-complemented pair EUFA316+FG, a positive control for FANCG expression). Extracts were separated by SDS-PAGE electrophoresis, followed by immunoblotting with antibodies against FANCG and nucleolin (NCL, a loading control). Two representative Western blot experiments are shown below, demonstrating ability of shFG31 and shFG32 to deplete FANCG protein from human cells.

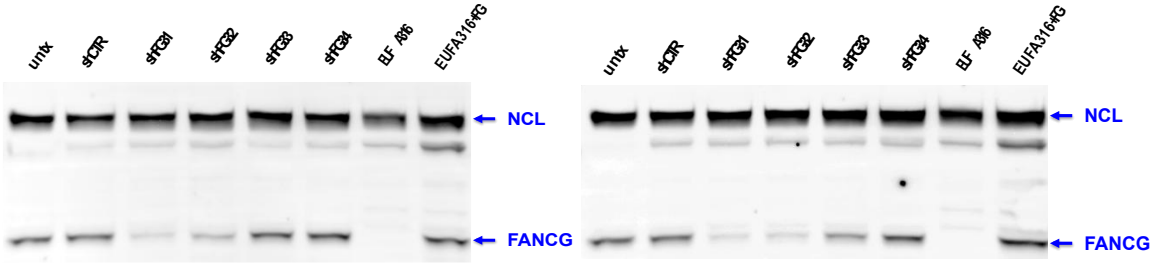

Expt. 1 **Expt. 2**

Detail of FANCG shRNAs:

shRNA:	shFG31	shFG32	*shCTR*
target sequence:	ggtagaattactactgccacc	ggtaatcgagacacttacttt	*gcttcgcgccgtagtctta*
target location:	nt 972-995 (ORF)	nt 1636-1657(ORF)	*n.a.(scrambled)*

Screen to identify shRNAs for human FANCA protein depletion: We screened 9 human *FANCA*-specific shRNAs from various sources to identify three that gave consistent, reproducible and substantial (≥90%) depletion of FANCG protein from human cells. Three of these (shFA31, shFA32, and shFA33, shown below), when transferred into and expressed from a lentiviral vector backbone, again were shown to reproducibly deplete FANCG protein to ≥90% from human cells.

***Western blot verification of FANCA depletion by shRNA*:** Whole cell lysates from U2-OS human osteosarcoma cells that were either untransduced (untx), transduced with and expressing a scrambled shRNA (shCTR), or transduced with and expressing one of 4 *FANCA*-targeting shRNAs (shFA31, shFA32, shFA33, and shFA34) were blotted with extracts from a control human FANCA-deficient lymphoblastoid cell line (HSC72, negative control for FANCA protein expression). Extracts were separated by SDS-PAGE electrophoresis, followed by immunoblotting with antibodies against FANCA and nucleolin (NCL, a loading control). A representative Western blot experiment is shown below, demonstrating ability of shFA31, shFA32 and shFA33 to deplete FANCG protein from human cells.

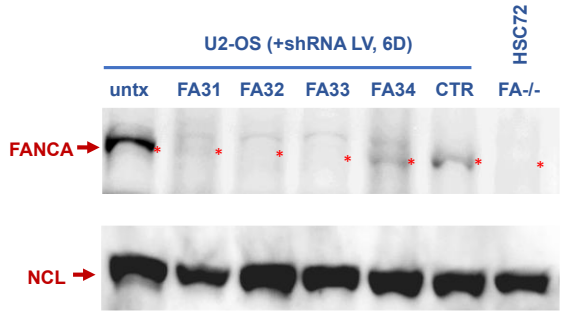

*: position of FANCA protein

Detail of FANCA shRNAs:

shRNA:	shFA32	*shFA33*	*shCTR*
target sequence:	ggtcttcctgtttacgttctt	*ggaagatgttcacttaactta*	*gcttcgcgccgtagtctta*
target location:	nt 1452-1472 (ORF)	*nt 2808-2828(ORF)*	*n.a.(scrambled)*

Lentivial transduction in CD34+ cells: Lentiviral shRNA vectors targeting *FANCA* (shFA32 and shFA33) and control scramble vector were produced in HEK293T, in CD34+ culture medium, using standard lentivirus packaging procedure. When transduced at a multiplicity of infection (MOI) of 10 with lentiviral vector alone or with the addition of 5µg/ml polybrene, very little transduction was observed (<0.1%, using mCherry reporter expression in the lentiviral vector as marker). When retronectin coated plates (Clontech, Mountview, CA) were used for transducing CD34+ cells at MOI=10, a significant improvement was observed and roughly 1-2% cells were transduced (as illustrated below, red indicates transduced CD34+ cells 4 days after transduction, superimposed with bright field image of all CD34+ cells). Attempts using either a higher MOI=20, or two sequential transductions, each at MOI=10, did not significantly increase transduction efficiency in CD34+ cells beyond retronectin treatment alone.

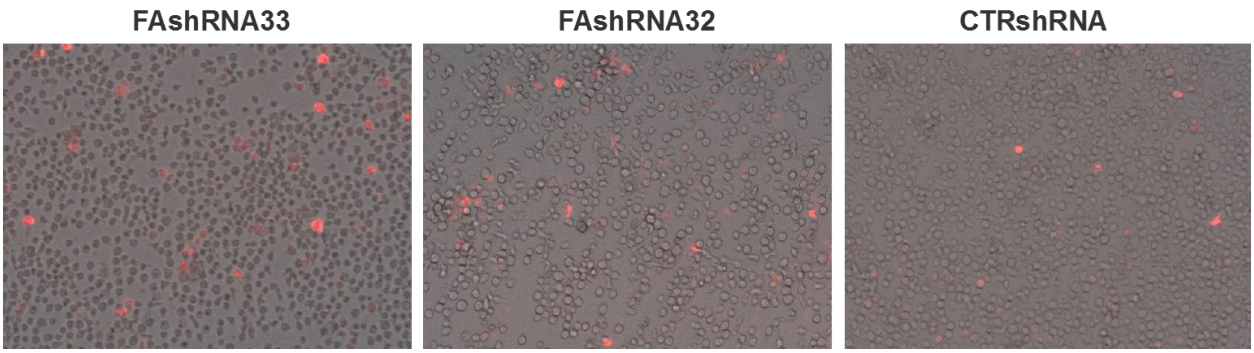

Aim 1 - Major Task 2: *In vitro* formaldehyde dose and small molecule protection of FANCG-depleted human CD34+ cells.

Small molecule protection of human cells from aldehyde-mediated cell killing: In conjunction with collaborators at Oregon Health Sciences University we demonstrated the ability of two small molecule protectants, metformin and aminoguanidine, to improve the growth, suppress aldehyde-induced DNA damage and improve the aldehyde dose-dependent survival of FANCG-deficient human cells.

Small molecules protection in vivo: We also showed that one of these small molecules, metformin, improves defective hematopoiesis and delays tumor formation in Fanconi anemia mice. This work, already published (see Zhang et al. (2016) Metformin improves defective hematopoiesis and delays tumor formation in Fanconi anemia mice. *Blood* DOI:10.1182/blood-2015-11-683490), provided critical pre-clinical data to inform a Phase I trial of the use of metformin to prevent the progression of bone marrow failure in Fanconi anemia patients. This manuscript identified this DoD-BMF award as one of the sources of research support.

Aim 2 - Major Task 1: Develop/validate stable isotope mass spec assay of formaldehyde DNA damage (in conjunction with collaborator James Swenberg/University of North Carolina).

Our collaborator Dr. James Swenberg completed the development of and published a new quantitative formaldehyde-DNA protein mass spectrometry-enabled assay in the past grant period: Lai et al. (2016) Measurement of endogenous versus exogenous formaldehyde-induced DNA-protein crosslinks in animal tissues by stable isotope labeling and ultrasensitive mass spectrometry. *Cancer Research* 76(9):2652-61. doi:10.1158/0008-5472.CAN-15-2527. PMC4879886.

Aim 2 - Major Task 2: Apply mass spectrometric assay to DNA derived from treated CD34+ cells (in conjunction with collaborator James Swenberg/University of North Carolina).

Dr. Swenberg also demonstrated with collaborator KJ Patel at the MRC Cambridge Lab of Molecular Biology the use of a related mass spectrometry-based method to detect and quantify DNA base adducts due to formaldehyde in *Adh5(-/-)Fancd2(-/-)* deficient mice and related control genotypes. This work has been published (Pontel et al. (2015) Endogenous formaldehyde is a hematopoietic stem cell genotoxin and metabolic carcinogen. *Molecular Cell* 60(1):177-88. doi: 10.1016/j.molcel.2015.08.020. PMC4595711).

Note: *Both of the above-cited publications are directly related to, and provide proof-of-concept for, our Revised Aim 2. The P.I. of this award, Dr. Monnat, originally connected Drs. Swenberg and Patel to foster the above-noted successful research collaboration and publication.*

– What opportunities for training and professional development has the project provided?

Development of the methods for the growth and depletion of FANCG protein from CD34+ cells provided a new opportunity for Dr. Tang in the Monnat Lab. In similar fashion the mass-spectrometry-based assay development providing training and development opportunities for members of the Swenberg Lab.

– Describe how the results were disseminated to communities of interest.

In addition to the publications cited above, this work was highlighted in platform talks at the 28th Annual Fanconi Anemia Research Fund Meeting that was held in Bellevue, WA on 15-18 September 2016. Dr. KJ Patel also gave a Keynote Address as part of this meeting entitled 'Aldehydes and the phenotype of Fanconi anemia: A complex illness with a simple explanation?' A full half-day session was also devoted to 'Aldehydes, Genotoxicity & Disease'.

– What do you plan to do during the next reporting period to accomplish the goals?

This is a final report for this award.

IMPACT:

As noted above, our results provide proof-of-concept of both biological as well as technical/methodology aspects of this project, and have provided key findings that provide the basis for early phase clinical trials of metformin in Fanconi anemia patients.

– What was the impact on other disciplines?

The fields of DNA damage-repair, DNA damage response, Fanconi anemia and associated bone marrow failure syndromes and environmental and molecular toxicology will all be interested in our newly generated data on the role of aldehydes, especially endogenous aldehydes generated as part of normal cellular metabolism, as an important source of DNA damage in human cells.

– What was the impact on technology transfer?

The mass spectrometry-based methods established in Dr. Swenberg's lab provide new tools for molecular assessment of aldehyde (and other types of) damage able to generate DNA base adducts or DNA-protein cross-links.

– Describe ways in which the project made an impact, or is likely to make an impact, on commercial technology or public use.

As noted above results of this research provide the basis for early phase clinical trials of the use of metformin to retard or suppress the progression of bone marrow failure in Fanconi anemia. We anticipate the eventual results may have utility in preventing or attenuating bone marrow failure in patients with Fanconi anemia, and potentially in other heritable or acquired bone marrow failure syndromes

CHANGES/PROBLEMS:

None – this is a final project report.

PRODUCTS:

- Publications, conference papers, and presentations

Please see our notes above on three related manuscripts, two supported in part by this award, together with presentations at the recent Fanconi Anemia Research Fund Symposium.

PARTICIPANTS & OTHER COLLABORATING ORGANIZATIONS

– What individuals have worked on the project?

Name: Ray Monnat
Project Role: Principal Investigator
Researcher Identifier (e.g. ORCID ID): 0000-0001-7638-7393
Nearest person month worked: 0.24 CM
Contribution to Project: design and conduct of experiments, interpretation of data, manuscript writing.
Funding Support: this award supported the above work

Name: Weiliang Tang
Project Role: Research Scientist
Researcher Identifier (e.g. ORCID ID): N/A
Nearest person month worked: 1 CM
Contribution to Project: design and conduct of experiments, interpretation of data
Funding Support: this award supported the above work

- Has there been a change in the active other support of the PD/PI(s) or senior/key personnel since the last reporting period?

No change in active support during the terminal award period.

– What other organizations were involved as partners?

University of North Carolina
Chapel Hill, NC

Collaborator James Swenberg and his lab are located at UNC-Chapel Hill. They have developed the mass spectrometric analytical methods to detect and quantify specific DNA base adducts and DNA-protein crosslinks, and have demonstrated the application of both methods in work now published (see above references).

SPECIAL REPORTING REQUIREMENTS:

Nothing to report.

COLLABORATIVE AWARDS:

Nothing to report.

For collaborative awards, independent reports are required from BOTH the Initiating PI and the Collaborating/Partnering PI. A duplicative report is acceptable; however, tasks shall be clearly marked with the responsible PI and research site. A report shall be submitted to https://ers.amedd.army.mil for each unique award.

QUAD CHARTS:

Nothing to report.

APPENDICES:

Copies of the following two publications are appended:

Zhang et al. (2016) Metformin improves defective hematopoiesis and delays tumor formation in Fanconi anemia mice. *Blood* 128(24):2774-2784. DOI:10.1182/blood-2015-11-683490. PMC5159699.

Lai et al. (2016) Measurement of endogenous versus exogenous formaldehyde-induced DNA-protein crosslinks in animal tissues by stable isotope labeling and ultrasensitive mass spectrometry. *Cancer Research* 76(9):2652-61. doi:10.1158/0008-5472.CAN-15-2527. PMC4879886.

Attach all appendices that contain information that supplements, clarifies or supports the text. Examples include original copies of journal articles, reprints of manuscripts and abstracts, a curriculum vitae, patent applications, study questionnaires, and surveys, etc. Reminder: Pages shall be consecutively numbered throughout the report. DO NOT RENUMBER PAGES IN THE APPENDICES.

Regular Article

blood

HEMATOPOIESIS AND STEM CELLS

Metformin improves defective hematopoiesis and delays tumor formation in Fanconi anemia mice

Qing-Shuo Zhang,[1] Weiliang Tang,[2] Matthew Deater,[1] Ngoc Phan,[1] Andrea N. Marcogliese,[3] Hui Li,[2] Muhsen Al-Dhalimy,[4] Angela Major,[5] Susan Olson,[4] Raymond J. Monnat Jr,[2,6] and Markus Grompe[1]

[1]Oregon Stem Cell Center, Department of Pediatrics, Oregon Health & Science University, Portland, OR; [2]Department of Pathology, University of Washington, Seattle, WA; [3]Department of Pathology, Baylor College of Medicine, TX; [4]Department of Molecular and Medical Genetics, Oregon Health & Science University, Portland, OR; [5]Department of Pathology, Texas Children's Hospital, Houston, TX; and [6]Department of Genome Sciences, University of Washington, Seattle, WA

Key Points

- The widely used diabetes drug metformin improves hematopoiesis and delays tumor formation in a preclinical murine model of FA.
- Metformin reduces DNA damage in human FA patient–derived cells.

Fanconi anemia (FA) is an inherited bone marrow failure disorder associated with a high incidence of leukemia and solid tumors. Bone marrow transplantation is currently the only curative therapy for the hematopoietic complications of this disorder. However, long-term morbidity and mortality remain very high, and new therapeutics are badly needed. Here we show that the widely used diabetes drug metformin improves hematopoiesis and delays tumor formation in *Fancd2*$^{-/-}$ mice. Metformin is the first compound reported to improve both of these FA phenotypes. Importantly, the beneficial effects are specific to FA mice and are not seen in the wild-type controls. In this preclinical model of FA, metformin outperformed the current standard of care, oxymetholone, by improving peripheral blood counts in *Fancd2*$^{-/-}$ mice significantly faster. Metformin increased the size of the hematopoietic stem cell compartment and enhanced quiescence in hematopoietic stem and progenitor cells. In tumor-prone *Fancd2*$^{-/-}$*Trp53*$^{+/-}$ mice, metformin delayed the onset of tumors and significantly extended the tumor-free survival time. In addition, we found that metformin and the structurally related compound aminoguanidine reduced DNA damage and ameliorated spontaneous chromosome breakage and radials in human FA patient–derived cells. Our results also indicate that aldehyde detoxification might be one of the mechanisms by which metformin reduces DNA damage in FA cells. (*Blood*. 2016; 128(24):2774-2784)

Introduction

Fanconi anemia (FA) is an inherited bone marrow failure disorder associated with a high incidence of leukemia and solid tumors.[1] The disorder is caused by a disrupted FA-BRCA pathway and is genetically heterogeneous, with at least 21 complementation groups and genes (*FANCA*, *FANCB*, *FANCC*, *FANCD1/BRCA2*, *FANCD2*, *FANCE*, *FANCF*, *FANCG*, *FANCI*, *FANCJ/BRIP1/BACH1*, *FANCL*, *FANCM*, *FANCN/PALB2*, *FANCO/RAD51C*, *FANCP/SLX4*, *FANCQ/XPF/ERCC4*, *FANCR/RAD51*, *FANCS/BRCA1*, *FANCT/UBE2T*, *FANCU/XRCC2*, and *FANCV/MAD2L2/REV7*) identified thus far. The main role of this gene network is to repair DNA lesions such as interstrand cross-links, which impede replication and transcription.[2,3]

The primary cause of early morbidity and mortality for FA patients is bone marrow failure.[4] Hematopoietic stem cells (HSCs) in FA patients are reduced in number, function poorly compared with healthy HSCs, and also suffer from progressive elimination because of the accumulation of unrepaired DNA damage.[5,6] Although most strains of FA mutant mice are poor models of the human disease, *Fancd2*$^{-/-}$ mice recapitulate the key human disease phenotypes well, including HSC defects and progressive bone marrow failure.[7,8] *Fancd2*$^{-/-}$ mice display thrombocytopenia by 3 to 6 months of age and eventually progress to peripheral pancytopenia by 18 months.[9] *Fancd2*$^{-/-}$ HSCs are less quiescent and show a severely reduced capacity to repopulate the hematopoietic system in vivo.[8]

The FA pathway plays a fundamental role in protecting cells against DNA damage–inducing aldehydes.[10] Disruption of key aldehyde detoxifying enzymes such as the aldehyde dehydrogenases Aldh2 or Adh5 in Fanconi mice induces phenotypes resembling clinical FA and leads to spontaneous bone marrow failure.[11,12] Of note, human FA patients carrying a dominant-negative allele of *ALDH2* demonstrate accelerated progression of bone marrow failure.[13] These observations suggest that attenuating aldehyde toxicity may provide a novel therapeutic approach to FA. Metformin (*N*,*N*-dimethylbiguanide) is a widely used drug to treat diabetes with proven safety after decades of clinical use.[14] As a guanidine derivative, metformin has the potential to scavenge DNA damage–inducing aldehydes through the Mannich reaction.[15] Metformin also induces the activation of adenosine 5′-monophosphate–activated protein kinase (AMPK) and is thought to have its antidiabetic effect via this mechanism.[16,17] We have reported

Submitted 23 November 2015; accepted 7 September 2016. Prepublished online as *Blood* First Edition paper, 18 October 2016; DOI 10.1182/blood-2015-11-683490.

The online version of this article contains a data supplement.

There is an Inside *Blood* Commentary on this article in this issue.

The publication costs of this article were defrayed in part by page charge payment. Therefore, and solely to indicate this fact, this article is hereby marked "advertisement" in accordance with 18 USC section 1734.

that the plant polyphenol resveratrol helps to restore the quiescence of *Fancd2*$^{-/-}$ HSCs and improves the function of hematopoietic stem and progenitor cells (HSPCs) in these mice.[8,18] Resveratrol has several bioactivities, including acting as an antioxidant, activating Sirt deacetylases (sirtuins), and activating AMPK.[19] However, we have recently demonstrated that a potent sirtuin activator, SRT3025, does not mimic the effects of resveratrol in FA mice.[20] Given that AMPK plays an important role in HSCs,[21] AMPK activation may be the primary mechanism by which resveratrol improves hematopoiesis. The ability of metformin to activate AMPK and act as a potential aldehyde scavenger makes metformin a potential candidate for the treatment of FA. In the current study, we tested the effects of chronic metformin therapy on hematopoiesis and cancer incidence in *Fancd2*$^{-/-}$ mice.

Materials and methods

Mice

Fancd2 mutant mice were maintained on the 129S4 background.[22] The metformin diet was made by milling metformin with standard rodent diet (Purina Chow 5001) at 3.75 g/kg diet (Bio-Serv, Flemington, NJ) and was administered to mice upon weaning (3-4 weeks of age). The treatment lasted 6 months unless specified otherwise. All animals were treated in accordance with the guidelines of the Institutional Animal Care and Use Committee.

Polyinosinic:polycytidylic acid [poly(I:C)] was purchased from GE Healthcare (Piscataway, NJ) and given to the mice at 8 mg/kg body weight via intraperitoneal injection. Control mice were injected with saline.

CBC

Blood samples were collected in EDTA-coated capillary tubes and complete blood counts (CBCs) were measured on a Hemavet 950FS Multi-species Hematology System (Drew Scientific, Inc, Dallas, TX).

Flow cytometry

Bone marrow cells were isolated from the femora and tibiae of mice and stained as described previously.[8] The c-Kit$^+$Sca-1$^+$Lin$^-$ (KSL) antibody cocktail was composed of anti-mouse c-Kit, Sca-1, and lineage markers (CD3e, CD4, CD5, CD8a, B220, Ter119, NK1.1, Mac1, and Gr1). For analysis of CD34$^-$KSL cells, nucleated bone marrow cells were stained with anti-mouse CD34 along with the KSL antibody cocktail. All the antibodies were from eBioscience (San Diego, CA). Flow cytometry analysis was performed on a Cytopeia Influx cell sorter.

CFU-S assay

Colony-forming unit–spleen (CFU-S) assay was performed as described previously[8] (see also supplemental Methods, available on the *Blood* Web site).

Cells and reagents

PD259i fibroblast cells, provided by the Oregon Health & Science University FA Cell Repository (http://www.ohsu.edu/research/fanconi-anemia/celllines.cfm), were originally derived from a human FA-A patient. EUFA316 lymphoblastoid cells were originally derived from a human FA-G patient.[23] EUFA316+FANCG cells were modified EUFA316 cells that stably express the wild-type FANCG.[24]

Metformin and aminoguanidine were purchased from MP Biomedicals (Santa Ana, CA) and Tokyo Chemical Industry (Tokyo, Japan), respectively. The Adh5 inhibitor C3 compound was obtained from ChemDiv (San Diego, CA).

Radial and chromosomal breakage assay

PD259i cells were treated with either metformin, aminoguanidine, or placebo. In the case when the C3 compound was used for the assay, C3 was added 1 hour after the addition of metformin. Forty-eight hours later, metaphase spreads were made and scored for radial contents and chromosomal breakage on a Zeiss Axioskop photoscope.

Statistical analysis

Unless specified otherwise, the 2-tailed, unpaired Student *t* test was used for statistical analysis. A value of $P < .05$ was considered significant.

Results

Dietary metformin administration enhances hematopoiesis

To determine whether metformin can influence hematopoiesis, cohorts of *Fancd2*$^{-/-}$ and wild-type mice were given either metformin-supplemented rodent chow or placebo for 6 months beginning at 1 month of age. The food intake was measured, and the effective dose via ingestion was calculated to be 300 mg/kg per day. On the basis of the body surface area conversion,[25] this dose was equivalent to only ~65% of the maximum dose used routinely in humans (~1300 mg/m^2). After 6 months, CBCs were examined. *Fancd2*$^{-/-}$ mice on the placebo diet showed mild pancytopenia in multiple lineages, including lower platelet counts, lower white and red blood cell counts, and lower hemoglobin levels than their wild-type gender-matched littermate placebo controls (Table 1). A CBC analysis revealed that chronic metformin treatment significantly increased platelet counts ($P < .05$; Figure 1A) in *Fancd2*$^{-/-}$ mice, but not in wild-type controls. In contrast, white blood cell counts ($P < .05$; Figure 1A) increased in both metformin-treated *Fancd2*$^{-/-}$ and wild-type mice. Although metformin-treated *Fancd2*$^{-/-}$ mice showed only a mild and non-significant increase in red blood cell number ($P = .08$; Figure 1A), the hemoglobin levels in metformin-treated *Fancd2*$^{-/-}$ mice were significantly higher than those in placebo-treated *Fancd2*$^{-/-}$ mice ($P < .005$; Figure 1A), nearly comparable to those observed in the placebo-treated wild-type controls. These multilineage improvements in hematologic parameters took place significantly faster with metformin treatment as opposed to oxymetholone treatment, the current standard androgen treatment of FA patients, on the same *Fancd2*$^{-/-}$ murine model tested in our previous studies.[9,20]

We next focused on characterizing the bone marrow of mice in this cohort. The marrow cellularity in either *Fancd2*$^{-/-}$ or wild-type mice was not different between metformin-treated animals and placebo-treated controls (data not shown). Interestingly, flow cytometry analysis demonstrated that the size of the CD34$^-$KSL cell compartment, an immunophenotypically defined HSC population in *Fancd2*$^{-/-}$ mice (Figure 1B), was significantly increased by 48% after 6 months of chronic metformin administration (Figure 1C). The size of the CD34$^-$ KSL cell compartment in wild-type mice, in contrast, was unchanged (Figure 1C), indicating that the effect of metformin on HSC population size was specific to *Fancd2*$^{-/-}$ mice.

Because our previous study showed that the AMPK activator resveratrol could help maintain stem cell quiescence in *Fancd2*$^{-/-}$ mice,[8] we measured the impact of metformin on the cell cycle status of HSPCs. The cell cycle profiles of KSL cells from metformin-treated mice were examined using Hoechst 33342 staining (for DNA content) and intracellular Ki67 staining (to discriminate cycling G1 cells from noncycling G0 cells).[26] As shown in Figure 2A-B, the average frequency of quiescent G0 KSL cells in metformin-treated *Fancd2*$^{-/-}$ mice was 27.4%, which was substantially higher ($P < .05$) than the average G0 fraction of 20.3% observed in placebo-treated gender-matched *Fancd2*$^{-/-}$ mice. Correspondingly, the average S-G2-M proportion of KSL cells in metformin-treated *Fancd2*$^{-/-}$ mice was

Table 1. CBCs in metformin-treated *Fancd2*$^{-/-}$ and *Fancd2*$^{+/+}$ mice

Blood counts	*Fancd2*$^{-/-}$ placebo	*Fancd2*$^{-/-}$ MET	*P*	*Fancd2*$^{+/+}$ placebo	*Fancd2*$^{+/+}$ MET	*P*	*P* (mutant placebo vs wild-type placebo)
WBCs, $\times 10^3/\mu L$	4.1 ± 0.2	5.1 ± 0.4	<.05	5.5 ± 0.4	6.8 ± 0.5	<.05	<.003
RBCs, $\times 10^6/\mu L$	8.9 ± 0.1	9.3 ± 0.2	.08	9.5 ± 0.1	9.7 ± 0.2	.24	<.01
Hb, g/dL	12.8 ± 0.1	13.5 ± 0.2	<.005	13.5 ± 0.2	13.6 ± 0.2	.80	<.003
HCT, %	49.5 ± 0.5	51.2 ± 0.8	.07	51.3 ± 0.8	51.6 ± 0.8	.76	.08
MCV, fL	55.6 ± 0.5	55.3 ± 0.3	.59	53.0 ± 0.3	53.4 ± 0.8	.49	<.0001
MCH, pg	14.4 ± 0.2	14.6 ± 0.1	.40	14.1 ± 0.2	14.0 ± 0.1	.52	.24
MCHC, g/dL	25.9 ± 0.2	26.3 ± 0.2	.16	26.6 ± 0.2	26.2 ± 0.1	.11	<.05
PLT, $\times 10^3/\mu L$	404 ± 17	465 ± 20	<.05	530 ± 19	562 ± 28	.37	<.0001

Data were pooled results from multiple mice (17-19 mice each group) and presented as mean value ± standard error of the mean.

Hb, hemoglobin; HCT, hematocrit; MCH, mean corpuscular hemoglobin; MCHC, mean corpuscular hemoglobin concentration; MCV, mean corpuscular volume; MET, metformin; PLT, platelet; RBC, red blood cell; WBC, white blood cell.

21.2%, which was significantly lower ($P < .05$) than the average S-G2-M percentage of 25.7% observed in placebo-treated controls. These results indicate that metformin treatment increased the quiescence of HSPCs in *Fancd2*$^{-/-}$ mice. In contrast, the cell cycle status of KSL cells in wild-type mice was unchanged after metformin treatment (Figure 2A-B).

Next, we performed the CFU-S assay, a short-term quantitative in vivo functional assay for HSPCs, using bone marrow from metformin-treated mice (Figure 3A). Metformin-treated *Fancd2*$^{-/-}$ bone marrow cells formed almost twice as many macroscopic splenic colonies ($P < .03$) as placebo-treated *Fancd2*$^{-/-}$ controls (Figure 3B), suggesting a marked improvement of HSPC function in metformin-treated *Fancd2*$^{-/-}$ bone marrow. In contrast, the CFU-S forming capacity in wild-type bone marrow was unchanged after metformin treatment ($P = .80$; Figure 3B).

Metformin administration protects FA cells from poly(I:C)-induced hematologic abnormalities

To further evaluate metformin's effects on hematopoiesis, we took advantage of the recent finding that HSC cycling induced by poly(I:C) in *Fanca*$^{-/-}$ mice caused aplastic anemia.[27] As depicted in Figure 3C, cohorts of 3-month-old *Fancd2*$^{-/-}$ mice and wild-type controls on metformin or placebo diet were given 3 consecutive high doses of poly(I:C) spaced 3 days apart. The mice were harvested 2 weeks after the completion of poly(I:C) treatment followed by analyses of bone marrow function. The CFU-S forming capacity of the bone marrow in *Fancd2*$^{-/-}$ mice was dramatically reduced after poly(I:C) administration ($P = .0001$; Figure 3D). Importantly, *Fancd2*$^{-/-}$ mice fed with a metformin diet while being given poly(I:C) displayed a complete protection from poly(I:C)-induced loss of HSPC activity, as evidenced by their maintenance of normal levels of CFU-S forming potential ($P < .01$; Figure 3D). This protection may reflect the ability of metformin to reenforce HSPC quiescence and hence counteract the deleterious effects of poly(I:C)-induced cycling on HSCs.

One characteristic FA patient phenotype, red cell deficiency, only becomes apparent in very old (18 months) *Fancd2*$^{-/-}$ mice.[9] However, only 3 weeks after poly(I:C) administration in 3-month-old *Fancd2*$^{-/-}$ mice, CBC analysis revealed a red cell deficiency and low hemoglobin levels ($P < .01$; Figure 3E). This effect was not observed in comparable control wild-type mice ($P = .35$). In a parallel study where *Fancd2*$^{-/-}$ mice were simultaneously fed with metformin while being given poly(I:C), metformin-fed mice displayed a clear protection from poly(I:C)-induced red cell deficiency ($P < .01$; Figure 3E). Collectively, these results indicate that metformin protects *Fancd2*$^{-/-}$ mice from poly(I:C)-induced hematologic abnormalities.

Metformin reduces DNA damage in FA cells

Because of a deficiency in interstrand cross-link repair, FA cells display high levels of radial chromosome formation and chromosomal breaks. These chromosomal changes are characteristic features of FA cells and are widely used to help confirm a clinical diagnosis of FA (Figure 4A).[28] Treatment with DNA cross-linking agents strongly induces this phenotype, but some FA cells also display spontaneously elevated chromosome breakage levels. We thus used this classic radial and breakage assay to determine whether metformin could protect FA cells from spontaneous DNA damage. FA-A patient–derived fibroblast cells (PD259i) that displayed spontaneous radials and breakage were treated with metformin (1 μM or 10 μM) for 48 hours before cytogenetic analysis. As shown in Figure 4B, metformin significantly reduced the levels of both radials and chromosomal breaks in PD259i cells, indicating that metformin can protect FA cells from developing DNA damage.

To better understand the mechanism behind this protective effect, we also tested another guanidine derivative, aminoguanidine, in the same assay. As shown in Figure 4C, aminoguanidine also significantly suppressed the formation of radials in PD259i cells, consistent with the chemical similarity and inferred mode of action of these 2 compounds.

Metformin may act by aldehyde detoxification

Increased sensitivity to DNA cross-linking agents such as formaldehyde and mitomycin C (MMC) is a characteristic hallmark of FA cells. Recent research has emphasized the role of endogenously produced aldehydes in producing DNA interstrand cross-links and contributing to the pathogenesis of bone marrow failure in FA.[10,11,13,29] In particular, endogenous formaldehyde, a highly reactive and abundant aldehyde generated by normal cellular processes such as DNA demethylation, has recently been shown to be an HSC genotoxin.[12] It is known that FA cells are sensitive to formaldehyde.[30] Consistent with these observations, we were able to demonstrate that cultured FA-G patient–derived lymphoblastoid cells (EUFA316) were sensitive to both the classic DNA cross-linking agent MMC and to formaldehyde (Figure 5A,C). Guanidine derivatives such as metformin and aminoguanidine have the ability to react with aldehydes through the Mannich reaction[15,31] and could potentially serve as aldehyde scavengers in FA cells to prevent DNA damage. Indeed, we found that aminoguanidine protected EUFA316 cells from dose-dependent, formaldehyde-induced growth arrest (Figure 5B). Surprisingly, we also observed a mild protection of aminoguanidine from MMC-induced growth arrest (Figure 5D).

To further assess whether metformin or aminoguanidine could protect FA-deficient cells, we devised a more sensitive cocultivation experiment in which equal numbers of EUFA316 cells and EUFA316+FANCG cells (stably complemented with a wild-type *FANCG* complementary DNA–encoding retrovirus) were labeled with different fluorescent proteins and allowed to compete in the presence of

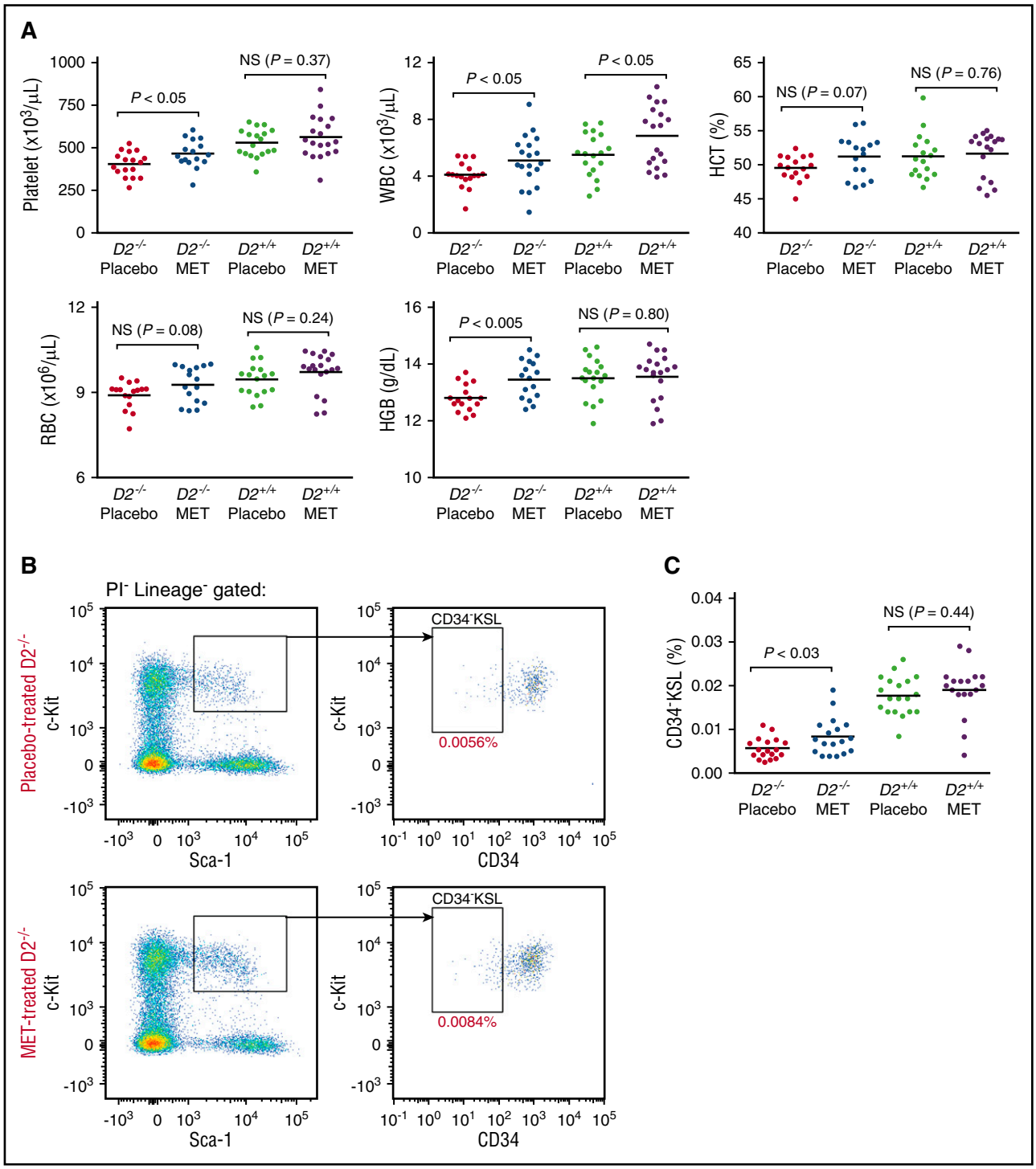

Figure 1. Metformin administration enhances hematopoiesis. (A) CBCs after 6 months of treatment with metformin. *D2*, *Fancd2*; HGB, hemoglobin; NS, not significant. The data are pooled results from 17 to 19 individual mice in each group. (B) Representative flow cytometry profiles for placebo and metformin-treated *Fancd2*$^{-/-}$ mice. The percentages on the profiles indicate the mean value for each group. PI, propidium iodide. (C) Quantification of CD34^{-}KSL frequency in bone marrow. The data represent the percentage of CD34^{-}KSL cells in all nucleated bone marrow cells from 15 mice in each group.

media only, 40 μM formaldehyde, or 6.25 nM MMC together with metformin or aminoguanidine (0.01, 0.1, or 1 mM). The competitive growth of these cells was monitored by flow cytometry. Both aminoguanidine and, to a lesser degree, metformin were able to provide dose-dependent protection against exogenous formaldehyde (supplemental Figure 1). We also observed protection against MMC by both aminoguanidine and metformin, although only at the highest dose tested (1 mM; supplemental Figure 1), probably reflecting the nonspecific protective effects of suppressed cell cycling by aminoguanidine or metformin. These results demonstrate that metformin and aminoguanidine protect FA-deficient cells from formaldehyde-induced and, to a much lesser extent, MMC-induced toxicity.

Formaldehyde is detoxified principally by formaldehyde dehydrogenase, encoded by the *Adh5/Gsnor* gene. *Adh5*$^{-/-}$ mice

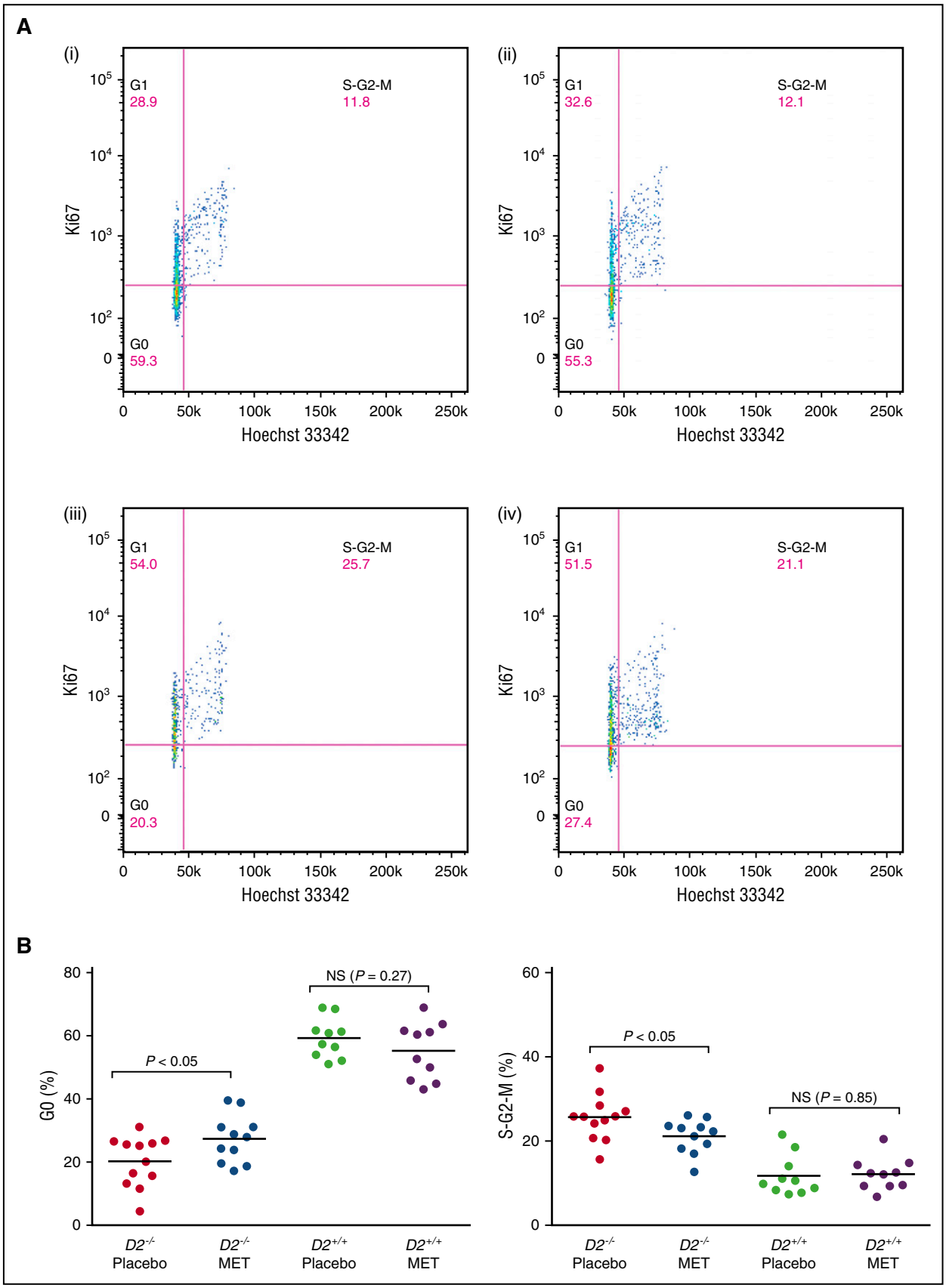

Figure 2. Metformin administration helps FA HSPCs maintain quiescence. (A) Representative flow cytometry profiles of the cell cycle analysis for KSL cells: placebo-treated *Fancd2*$^{+/+}$ KSL cells (i), MET-treated *Fancd2*$^{+/+}$ KSL cells (ii), placebo-treated *Fancd2*$^{-/-}$ KSL cells (iii), and MET-treated *Fancd2*$^{-/-}$ KSL cells (iv). The percentages on the profiles indicate the mean value for each group. (B) Statistical analysis of the cell cycle status. Data are poled results from 10 to 15 mice.

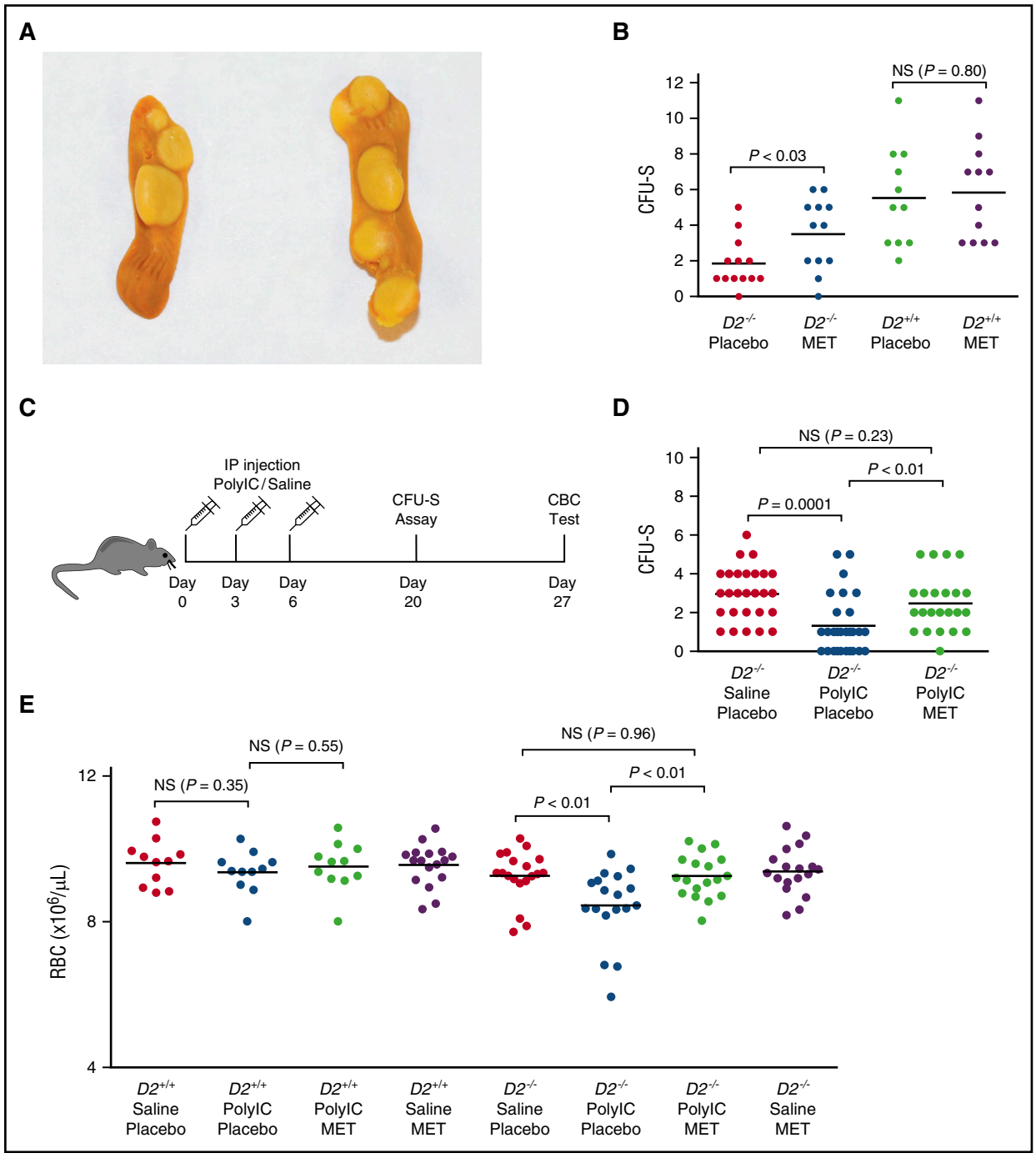

Figure 3. Metformin administration improves the function of FA bone marrow cells. (A) Representative pictures of spleens analyzed in the CFU-S assay. (B) Statistical analysis of CFU-S assays. Forty thousand donor bone marrow cells were injected intravenously into each recipient mouse. Data represent 3 or 4 donors in each group of mice, with 2 to 4 recipients for each donor. (C) Schematic chart to show the procedures of poly(I:C) experiments. Three-month-old mice were injected intraperitoneally with either poly(I:C) or saline at 8 mg/kg body weight. The mice were harvested either 2 weeks (for CFU-S assay) or 3 weeks (for CBC analysis) after the completion of poly(I:C) treatment. (D) Statistical analysis of CFU-S assays after poly(I:C) administration. Data represent 8 or 9 donors in each group of mice, with 2 to 4 recipients for each donor. Total recipients in each group ranged from 23 to 28 mice. (E) Statistical analysis of CBC tests after poly(I:C) administration. Data are pooled results from 11 to 17 mice each group for wild-type mice and 18 to 19 mice each group for *Fancd2*$^{-/-}$ mice.

accumulate formaldehyde adducts in DNA.[12] To determine whether metformin was able to suppress formaldehyde-induced DNA damage, we used a recently discovered small-molecule inhibitor of Adh5, the C3 compound, to induce the accumulation of endogenous formaldehyde in FA cells.[32,33] After human FA-A patient–derived fibroblast cells PD259i were treated with 100 μM C3 for 48 hours, the levels of spontaneous radials and chromosomal breaks were significantly increased by twofold and threefold, respectively ($P < .0001$ in both cases; Figure 5E-F). Importantly, concurrent treatment with metformin significantly suppressed C3-induced radials and chromosomal breaks ($P < .0001$ and $P < .001$, respectively; Figure 5E-F), consistent with a role for metformin in detoxifying formaldehyde.

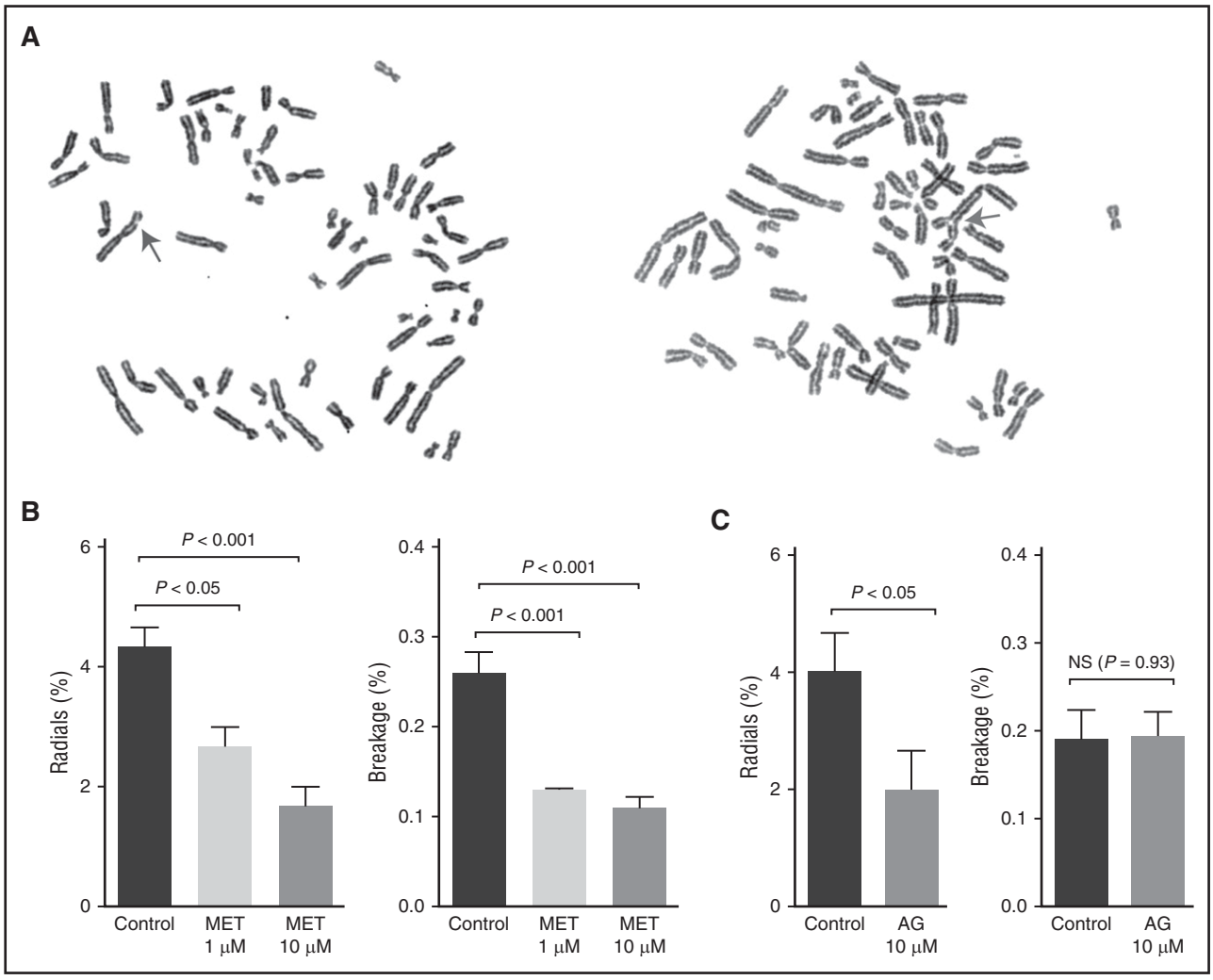

Figure 4. Metformin prevents FA patient–derived cells from developing radials and chromosomal breaks. (A) Representative pictures of spontaneous radials and breaks in PD259i human FA-A fibroblasts. The arrows indicate a chromosomal break (left) or a radial (right). (B-C) Statistical quantitation of radials and breaks in PD259i human FA-A fibroblasts after aminoguanidine or metformin treatment. PD259i cells were maintained in DMEM supplemented with 10% fetal bovine serum and penicillin/streptomycin. Cells were cultured with metformin or aminoguanidine for 48 hours before metaphase spreads were made. Fifty metaphases for each sample were scored for radial contents and chromosomal breakage. Data are combined results from 6 independent experiments. AG, aminoguanidine.

Metformin delays tumor formation in *Fancd2*$^{-/-}$ mice

The in vitro experiments above showed that metformin could reduce spontaneous DNA damage in FA cells. In addition, metformin is well known to reduce the incidence of several human cancers.[34,35] For these reasons, metformin was tested as a cancer chemopreventive agent. A cohort of tumor prone *Fancd2*$^{-/-}$*Trp53*$^{+/-}$ mice along with *Fancd2*$^{+/+}$ *Trp53*$^{+/-}$ littermate controls were divided into 2 groups and treated with either metformin or placebo diet. The tumor spectrum in metformin-treated *Fancd2*$^{-/-}$*Trp53*$^{+/-}$ mice was similar to that in placebo-treated controls. The most common type of tumor was ovarian in origin, consistent with our previous observation on tumor types in *Fancd2*$^{-/-}$ mice[9,22] and an earlier study reporting that more than 18% of human primary ovarian epithelial cancers have a disrupted FA/BRCA pathway.[36] Specifically, 61 *Fancd2*$^{-/-}$*Trp53*$^{+/-}$ mice under placebo treatment developed 91 tumors, among which 37 (41%) were ovarian tumors; 31 *Fancd2*$^{-/-}$*Trp53*$^{+/-}$ mice under metformin treatment developed 34 tumors, among which 13 (38%) were ovarian tumors. These spectra were similar to what we have reported before.[37] However, as shown in Figure 6, *Fancd2*$^{-/-}$*Trp53*$^{+/-}$ mice on metformin diet showed a significantly longer ($P < .05$) mean tumor-free survival time (mean survival of 405 days) than the *Fancd2*$^{-/-}$*Trp53*$^{+/-}$ mice on placebo diet (mean survival of 368 days). The first tumor was seen at 142 days in the *Fancd2*$^{-/-}$ *Trp53*$^{+/-}$ mice on placebo diet, whereas the earliest tumor in the *Fancd2*$^{-/-}$*Trp53*$^{+/-}$ mice on metformin appeared much later at 244 days of age. Overall, these results indicate that metformin administration significantly delays tumor formation in *Fancd2*$^{-/-}$*Trp53*$^{+/-}$ mice.

In contrast, as shown in Figure 6, the *Fancd2*$^{+/+}$*Trp53*$^{+/-}$ mice on placebo diet had a mean tumor-free survival of 510 days, and those on metformin diet survived an average of 535 days. There was no significant difference between metformin and placebo treatment in these p53 heterozygotes ($P = .86$), indicating that the tumor-delaying effect of metformin was specific to only FA mutant mice.

Discussion

The majority of genes responsible for FA have now been found and many of their biochemical functions are being uncovered.[2,3] The FA

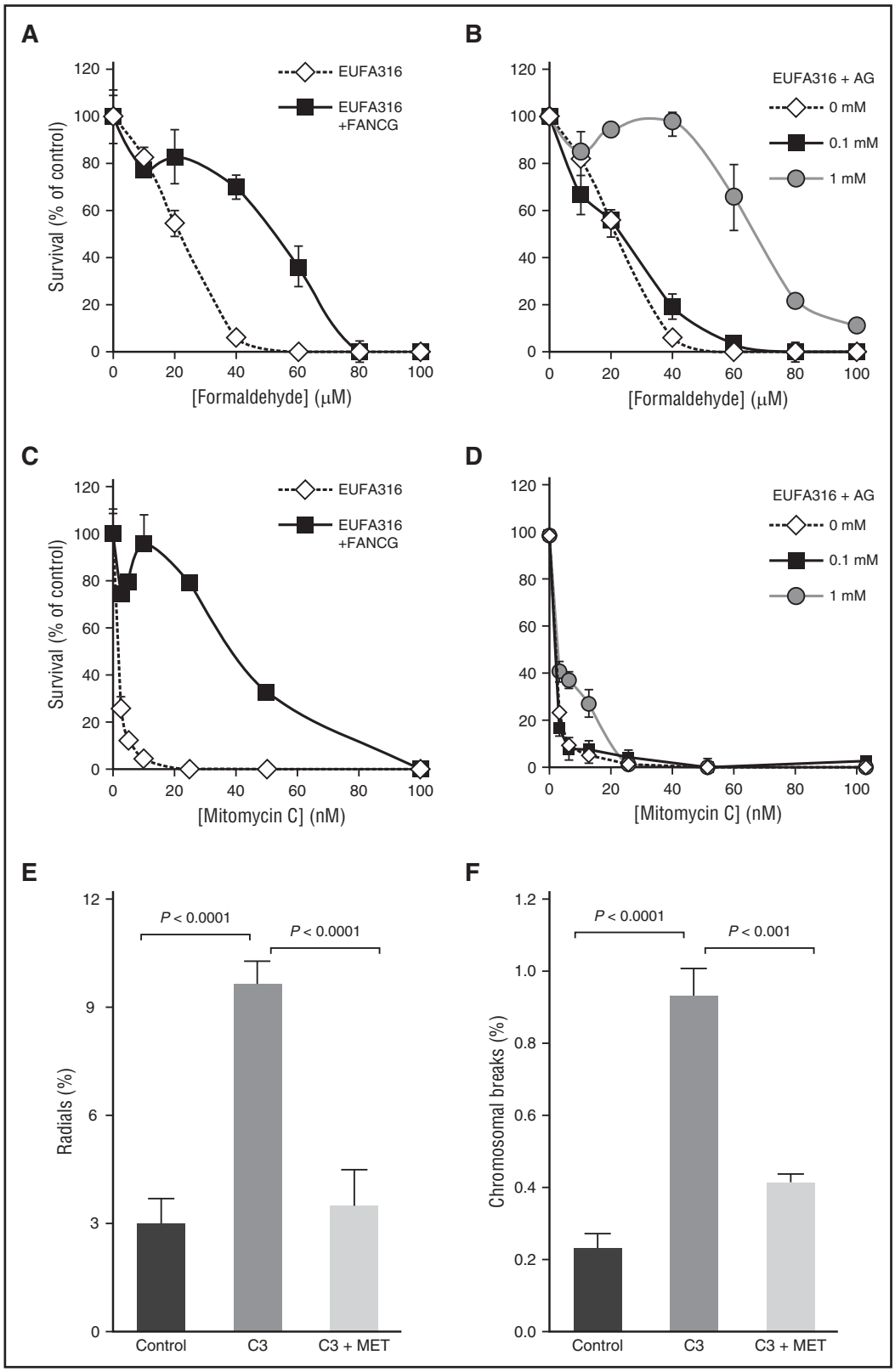

Figure 5. Aldehyde sensitivity of human FA cells and the detoxification of aldehydes by aminoguanidine. (A) Formaldehyde dose-dependent survival of EUFA316 human FA-G mutant lymphoblastoid cells compared with an isogenic, FANCG-complemented EUFA316 control. Complementation of patient cells was performed by stably transducing FANCG-mutant EUFA316 cells with a retrovirus expressing a wild-type human *FANCG* complementary DNA. EUFA316 and EUFA316+FANCG cells were cultivated in RPMI 1640 medium supplemented with 10% fetal bovine serum and penicillin/streptomycin. (B) Aminoguanidine shows dose-dependent rescue of EUFA316 cells from formaldehyde-induced cell death. (C) MMC dose-dependent survival of EUFA316 and wild-type controls. (D) Aminoguanidine provided a mild protection on EUFA316 cells from MMC-induced cell death. (E-F) Statistical quantitation of radials and chromosomal breaks in 259i human FA-A fibroblasts treated with C3, the ADH5 inhibitor. Metformin was added to the cell culture at 10 μM and maintained at the same concentration throughout the experiment. One hour later, C3 was added at 100 μM. Forty-eight hours later, cells were harvested for breakage and radial analysis. Data are combined results from 4 independent experiments.

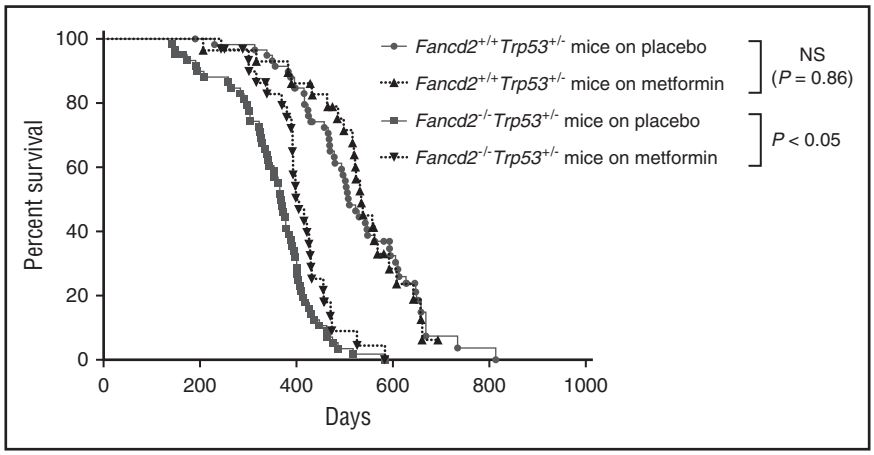

Figure 6. Metformin protects *Fancd2*$^{-/-}$ mice from tumor development. Kaplan-Meier survival curves of the *Fancd2*$^{-/-}$*Trp53*$^{+/-}$ mice and *Fancd2*$^{+/+}$*Trp53*$^{+/-}$ mice. For *Fancd2*$^{-/-}$*Trp53*$^{+/-}$ mice, the data represent 31 mice for metformin treatment and 60 mice for placebo treatment. For *Fancd2*$^{+/+}$*Trp53*$^{+/-}$ mice, the data represent 30 mice for metformin treatment and 60 mice for placebo treatment. Tumor samples and selected tissues were fixed in 10% phosphate-buffered formalin, stained with hematoxylin and eosin, and examined under a microscope. The Kaplan-Meier survival curves were generated by Prism 6.0c Software (GraphPad Software, Inc.), and *P* values were calculated using the log-rank (Mantel-Cox) test.

network consists of at least 21 proteins that serve to maintain genome stability, enhance stem cell survival, and suppress cancer and are functionally integrated with genes involved in inherited breast and ovarian cancers (eg, *BRCA1* and *BRCA2*). Despite these scientific insights, there has been little progress in treating human FA patients or preventing bone marrow failure. Bone marrow transplantation is currently the only curative therapy for the hematopoietic complications of the disorder, but when performed without a matched sibling donor, it is often accompanied by both short-term and long-term morbidities.[1] Among these complications is a very high risk of secondary cancer.[38] Synthetic androgens have been used for many years to support marrow function and improve cytopenias for a subset of FA patients.[39,40] However, these outcomes are limited by incomplete or transient responses, together with unacceptable side effects and toxicities. Gene therapy remains a promising approach for FA,[41] but to date there have been no reports of clinical success despite the selective advantage for gene corrected stem cells in this disorder. Furthermore, as noted previously, successful treatment of bone marrow failure does not diminish the severity or risk of nonhematopoietic consequences of FA, most notably the high risk of solid tumors.[38] New therapeutic approaches that have the ability to treat or prevent bone marrow failure and cancer are thus clearly needed for FA.[8,9,20,37,42]

Here we show that the widely used diabetes drug metformin improves hematopoiesis and delays tumor formation in *Fancd2*$^{-/-}$ mutant mice. Of note, metformin is the first compound to improve both of these FA phenotypes: oxymetholone,[9] resveratrol,[8] sirtuin activator,[20] and *N*-acetylcysteine[42] all improve hematopoiesis in *Fancd2*$^{-/-}$ mice, but none has been shown to diminish tumor incidence. In contrast, the antioxidant tempol delays cancer in FA but does not benefit hematopoiesis.[37] Our results indicate that metformin can ameliorate both of these key phenotypes of FA, and that its beneficial action was specific to FA mutant mice. In contrast, oxymetholone and the sirtuin activator SRT3025 affect both wild-type and mutant stem cells equally,[9,20] indicating that their mechanisms of action do not target the pathophysiology of FA bone marrow failure. Furthermore, it is particularly intriguing that the chronic administration of metformin significantly increases the frequency of HSCs in the adult *Fancd2*$^{-/-}$ mice. The loss of HSCs in FA lies at the root of bone marrow failure and is a progressive process that extends from adolescence into adulthood.[5,6,9] There is an emerging body of evidence supporting that this progressive HSC loss may begin in utero.[8,43,44] Although the magnitude of HSC rescue by metformin is relatively small, this drug demonstrates a unique ability to restore the HSC numbers in postnatal life in FA mice.

The specificity of action of metformin and the structurally related compound aminoguanidine in the protection of FA mutant cells may be explained by our observation that both compounds appear to selectively reduce DNA damage in FA cells. This is demonstrated by the dose-dependent reduction of spontaneous radial chromosome formation and chromosome breaks in a human FA cell line treated with either compound.

The precise mechanism by which metformin and aminoguanidine reduce DNA damage in FA cells remains unclear, although here we present evidence that aldehyde detoxification may be an important part of the protective effect conferred by both metformin and aminoguanidine. Endogenously produced aldehydes, including acetaldehyde and formaldehyde, are clearly genotoxic in FA mutant cells.[11,12,29,45] We found that the pharmacological inhibition of Adh5, the main enzyme responsible for cellular formaldehyde detoxification, induced chromosome breakage and radials in FA cells. Importantly, metformin rescued this defect at physiologically relevant concentrations. Given that the chemically related guanidine derivative aminoguanidine was also able to block formaldehyde toxicity, presumably through the well-described Mannich reaction,[15,31] our data are consistent with the hypothesis that metformin acts at least in part through an aldehyde scavenging mechanism. It is surprising that metformin also mildly protected FA patient cells from MMC-induced growth arrest. This could be because of the release of lipid peroxidation–derived aldehyde 4-hydroxy-2-nonenal associated with MMC treatment[46] and/or methanol (which could be oxidized to formaldehyde) during the activation of MMC.[47] However, it is also possible that metformin may act via other mechanisms to attenuate the FA phenotype. For example, metformin potently activates AMPK, a kinase known to be important in protecting HSCs from genomic instability.[21] Of note, in our previous transcriptome analysis of HSPCs,[9] the messenger RNA encoding *SLC22A3*, one of the membrane transporters important for metformin uptake,[34,48] is preferentially enriched by 12.3-fold in HSPCs, as compared with whole bone marrow cells. It is thus possible that metformin can exert its effects directly on HSPCs. Metformin's effects on the *Fancd2*$^{-/-}$ hematopoietic system, including reenforcing quiescence in HSPCs and increasing CFU-S–forming capacity of bone marrow cells, resemble the effects of resveratrol,[8] another known AMPK activator.[19] It is, therefore, tempting to suggest that metformin and resveratrol might exert their hematopoietic benefits through the AMPK signaling pathway. However, this does not explain all the effects from metformin because metformin delays tumor formation in *Fancd2*$^{-/-}$ mice, whereas resveratrol does not. We recently discovered that transforming growth factor β (TGF-β) inhibitors can protect HSCs in FA mice and patients by altering the

balance of nonhomologous end joining and homologous recombination.[49] Although metformin is not known to directly interfere with TGF-β signaling, several reports indicate interactions between the LKB1/AMPK pathways and TGF-β.[50] Other mechanisms by which metformin may act to protect FA mice include the following: reducing the activity of mitochondrial complex 1 activity,[14] thus potentially reducing oxidative DNA damage[51,52]; supporting the expansion of HSCs in vitro by switching the metabolic balance between oxidative phosphorylation and anaerobic glycolysis[53]; and downregulating inflammatory pathways,[54] which are thought to contribute to bone marrow failure in FA.[55] Future studies will be needed to determine whether 1 or more of these known mechanisms in addition to aldehyde quenching are responsible for the beneficial effects of metformin in FA.

Despite these uncertainties as to the exact mechanism of protection by metformin, a compelling argument can be made for a clinical trial of metformin to protect FA patients from bone marrow failure and tumorigenesis. Metformin has a superb safety record in light of its wide clinical use to treat diabetes mellitus over >2 decades. In our preclinical model, metformin outperforms the current standard of care, oxymetholone. Oxymetholone therapy had no significant effect on peripheral blood counts of FA mice at 6 months.[20] Its benefits only became apparent after 17 months of treatment.[9] In contrast, metformin improved peripheral blood counts after only 6 months of therapy.

Several important questions remain to be answered. The optimal dose of metformin for FA therapy and disease prevention is not known. If metformin acts predominantly as an aldehyde scavenger, higher doses may be optimal, and a well-tolerated high dose could be readily determined from use and toxicity data. It is also not known when beginning metformin treatment would be most beneficial: prior to the onset of bone marrow failure or only after the development of anemia. Finally, potential synergies between metformin and anabolic androgens, the current gold standard of therapy, have not been studied. These interactions are difficult to predict directly, as androgens accelerate the cell cycle of stem cells,[9] whereas metformin increases quiescence.

Our results may also have relevance in regard to the use of metformin in the general population as an antiaging and cancer chemoprevention drug.[56] Metformin has not previously been reported to protect the genome from DNA damage and mutation. However, such activity would go a long way toward explaining why it can.

Acknowledgments

The authors thank Pamela Canady and Mandy Boyd at the Oregon Health & Science University flow cytometry core for fluorescence-activated cell sorting, William H. Fleming and Devorah C. Goldman for valuable advice, and Laura Marquez-Loza for help with animal care.

This work was supported by the National Heart, Lung, and Blood Institute, National Institutes of Health National Heart, Lung, and Blood Institute (grant P01 HL048546) (M.G.), the Fanconi Anemia Research Foundation (M.G.), and an award from the Office of the Assistant Secretary of Defense for Health Affairs, through the Bone Marrow Failure Research Program (award no. W81XWH-14-1-0297) (R.J.M.).

Authorship

Contribution: Q.-S.Z. designed the study, performed research, analyzed and interpreted the data, and wrote the manuscript; M.D., N.P., W.T., H.L., M.A.-D., and A.M. performed research; R.J.M. and S.O. designed the in vitro studies, interpreted the data, and wrote the manuscript; A.N.M. examined the histological slides and wrote the manuscript; and M.G. designed the study, analyzed and interpreted the data, and wrote the manuscript.

Conflict-of-interest disclosure: The authors declare no competing financial interests.

The current affiliation for H.L. is Department of Anatomy and Neurobiology, Northeastern Ohio Medical University, Rootstown, OH.

ORCID profiles: Q.-S.Z., 0000-0002-4407-6053; M.G., 0000-0002-6616-4345.

Correspondence: Qing-Shuo Zhang, Oregon Stem Cell Center, Department of Pediatrics, Oregon Health & Science University, 3181 SW Sam Jackson Park Rd, Portland, OR 97239; e-mail: zhangqi@ohsu.edu.

References

1. Shimamura A, Alter BP. Pathophysiology and management of inherited bone marrow failure syndromes. *Blood Rev*. 2010;24(3):101-122.
2. Kim H, D'Andrea AD. Regulation of DNA cross-link repair by the Fanconi anemia/BRCA pathway. *Genes Dev*. 2012;26(13):1393-1408.
3. Kottemann MC, Smogorzewska A. Fanconi anaemia and the repair of Watson and Crick DNA crosslinks. *Nature*. 2013;493(7432):356-363.
4. Kutler DI, Singh B, Satagopan J, et al. A 20-year perspective on the International Fanconi Anemia Registry (IFAR). *Blood*. 2003;101(4):1249-1256.
5. Ceccaldi R, Parmar K, Mouly E, et al. Bone marrow failure in Fanconi anemia is triggered by an exacerbated p53/p21 DNA damage response that impairs hematopoietic stem and progenitor cells. *Cell Stem Cell*. 2012;11(1):36-49.
6. Kelly PF, Radtke S, von Kalle C, et al. Stem cell collection and gene transfer in Fanconi anemia. *Mol Ther*. 2007;15(1):211-219.
7. Parmar K, Kim J, Sykes SM, et al. Hematopoietic stem cell defects in mice with deficiency of Fancd2 or Usp1. *Stem Cells*. 2010;28(7):1186-1195.
8. Zhang QS, Marquez-Loza L, Eaton L, et al. Fancd2-/- mice have hematopoietic defects that can be partially corrected by resveratrol. *Blood*. 2010;116(24):5140-5148.
9. Zhang QS, Benedetti E, Deater M, et al. Oxymetholone therapy of fanconi anemia suppresses osteopontin transcription and induces hematopoietic stem cell cycling. *Stem Cell Rep*. 2015;4(1):90-102.
10. Langevin F, Crossan GP, Rosado IV, Arends MJ, Patel KJ. Fancd2 counteracts the toxic effects of naturally produced aldehydes in mice. *Nature*. 2011;475(7354):53-58.
11. Garaycoechea JI, Crossan GP, Langevin F, Daly M, Arends MJ, Patel KJ. Genotoxic consequences of endogenous aldehydes on mouse haematopoietic stem cell function. *Nature*. 2012;489(7417):571-575.
12. Pontel LB, Rosado IV, Burgos-Barragan G, et al. Endogenous formaldehyde is a hematopoietic stem cell genotoxin and metabolic carcinogen. *Mol Cell*. 2015;60(1):177-188.
13. Hira A, Yabe H, Yoshida K, et al. Variant ALDH2 is associated with accelerated progression of bone marrow failure in Japanese Fanconi anemia patients. *Blood*. 2013;122(18):3206-3209.
14. Foretz M, Guigas B, Bertrand L, Pollak M, Viollet B. Metformin: from mechanisms of action to therapies. *Cell Metab*. 2014;20(6):953-966.
15. Kazachkov M, Chen K, Babiy S, Yu PH. Evidence for in vivo scavenging by aminoguanidine of formaldehyde produced via semicarbazide-sensitive amine oxidase-mediated deamination. *J Pharmacol Exp Ther*. 2007;322(3):1201-1207.
16. Viollet B, Guigas B, Sanz Garcia N, Leclerc J, Foretz M, Andreelli F. Cellular and molecular mechanisms of metformin: an overview. *Clin Sci (Lond)*. 2012;122(6):253-270.
17. Zhou G, Myers R, Li Y, et al. Role of AMP-activated protein kinase in mechanism of metformin action. *J Clin Invest*. 2001;108(8):1167-1174.
18. Park SJ, Ahmad F, Philp A, et al. Resveratrol ameliorates aging-related metabolic phenotypes by inhibiting cAMP phosphodiesterases. *Cell*. 2012;148(3):421-433.
19. Lagouge M, Argmann C, Gerhart-Hines Z, et al. Resveratrol improves mitochondrial function and protects against metabolic disease by activating SIRT1 and PGC-1alpha. *Cell*. 2006;127(6):1109-1122.
20. Zhang QS, Deater M, Schubert K, et al. The Sirt1 activator SRT3025 expands hematopoietic stem and progenitor cells and improves hematopoiesis in Fanconi anemia mice. *Stem Cell Res (Amst)*. 2015;15(1):130-140.

21. Nakada D, Saunders TL, Morrison SJ. Lkb1 regulates cell cycle and energy metabolism in haematopoietic stem cells. *Nature*. 2010; 468(7324):653-658.
22. Houghtaling S, Timmers C, Noll M, et al. Epithelial cancer in Fanconi anemia complementation group D2 (Fancd2) knockout mice. *Genes Dev*. 2003; 17(16):2021-2035.
23. de Winter JP, Waisfisz Q, Rooimans MA, et al. The Fanconi anaemia group G gene FANCG is identical with XRCC9. *Nat Genet*. 1998;20(3): 281-283.
24. Garcia-Higuera I, Kuang Y, Näf D, Wasik J, D'Andrea AD. Fanconi anemia proteins FANCA, FANCC, and FANCG/XRCC9 interact in a functional nuclear complex. *Mol Cell Biol*. 1999; 19(7):4866-4873.
25. Reagan-Shaw S, Nihal M, Ahmad N. Dose translation from animal to human studies revisited. *FASEB J*. 2008;22(3):659-661.
26. Wilson A, Laurenti E, Oser G, et al. Hematopoietic stem cells reversibly switch from dormancy to self-renewal during homeostasis and repair. *Cell*. 2008;135(6):1118-1129.
27. Walter D, Lier A, Geiselhart A, et al. Exit from dormancy provokes DNA-damage-induced attrition in haematopoietic stem cells. *Nature*. 2015;520(7548):549-552.
28. Auerbach AD. Fanconi anemia and its diagnosis. *Mutat Res*. 2009;668(1-2):4-10.
29. Rosado IV, Langevin F, Crossan GP, Takata M, Patel KJ. Formaldehyde catabolism is essential in cells deficient for the Fanconi anemia DNA-repair pathway. *Nat Struct Mol Biol*. 2011;18(12): 1432-1434.
30. Ridpath JR, Nakamura A, Tano K, et al. Cells deficient in the FANC/BRCA pathway are hypersensitive to plasma levels of formaldehyde. *Cancer Res*. 2007;67(23):11117-11122.
31. Roman G. Mannich bases in medicinal chemistry and drug design. *Eur J Med Chem*. 2015;89: 743-816.
32. Sanghani PC, Davis WI, Fears SL, et al. Kinetic and cellular characterization of novel inhibitors of S-nitrosoglutathione reductase. *J Biol Chem*. 2009;284(36):24354-24362.
33. Wu K, Ren R, Su W, et al. A novel suppressive effect of alcohol dehydrogenase 5 in neuronal differentiation. *J Biol Chem*. 2014;289(29): 20193-20199.
34. Pernicova I, Korbonits M. Metformin–mode of action and clinical implications for diabetes and cancer. *Nat Rev Endocrinol*. 2014;10(3):143-156.
35. Taubes G. Cancer research. Cancer prevention with a diabetes pill? *Science*. 2012;335(6064):29.
36. Taniguchi T, Tischkowitz M, Ameziane N, et al. Disruption of the Fanconi anemia-BRCA pathway in cisplatin-sensitive ovarian tumors. *Nat Med*. 2003;9(5):568-574.
37. Zhang QS, Eaton L, Snyder ER, et al. Tempol protects against oxidative damage and delays epithelial tumor onset in Fanconi anemia mice. *Cancer Res*. 2008;68(5):1601-1608.
38. Alter BP, Greene MH, Velazquez I, Rosenberg PS. Cancer in Fanconi anemia. *Blood*. 2003; 101(5):2072.
39. Rose SR, Kim MO, Korbee L, et al. Oxandrolone for the treatment of bone marrow failure in Fanconi anemia. *Pediatr Blood Cancer*. 2014; 61(1):11-19.
40. Velazquez I, Alter BP. Androgens and liver tumors: Fanconi's anemia and non-Fanconi's conditions. *Am J Hematol*. 2004;77(3):257-267.
41. Tolar J, Becker PS, Clapp DW, et al. Gene therapy for Fanconi anemia: one step closer to the clinic. *Hum Gene Ther*. 2012;23(2):141-144.
42. Zhang QS, Marquez-Loza L, Sheehan AM, et al. Evaluation of resveratrol and N-acetylcysteine for cancer chemoprevention in a Fanconi anemia murine model. *Pediatr Blood Cancer*. 2014;61(4): 740-742.
43. Kamimae-Lanning AN, Goloviznina NA, Kurre P. Fetal origins of hematopoietic failure in a murine model of Fanconi anemia. *Blood*. 2013;121(11): 2008-2012.
44. Liu TX, Howlett NG, Deng M, et al. Knockdown of zebrafish Fancd2 causes developmental abnormalities via p53-dependent apoptosis. *Dev Cell*. 2003;5(6):903-914.
45. Oberbeck N, Langevin F, King G, de Wind N, Crossan GP, Patel KJ. Maternal aldehyde elimination during pregnancy preserves the fetal genome. *Mol Cell*. 2014;55(6):807-817.
46. Matsunaga T, Yamane Y, Iida K, et al. Involvement of the aldo-keto reductase, AKR1B10, in mitomycin-c resistance through reactive oxygen species-dependent mechanisms. *Anticancer Drugs*. 2011;22(5):402-408.
47. Dobrowsky W. Mitomycin C and radiotherapy. In: Huilgol NG, Nair CKK, Kagiya VT, eds. Radiation Sensitizers: A Contemporary Audit. Boca Raton, FL: CRC Press; 2001:26-32.
48. Chen L, Pawlikowski B, Schlessinger A, et al. Role of organic cation transporter 3 (SLC22A3) and its missense variants in the pharmacologic action of metformin. *Pharmacogenet Genomics*. 2010;20(11):687-699.
49. Zhang H, Kozono DE, O'Connor KW, et al. TGF-β inhibition rescues hematopoietic stem cell defects and bone marrow failure in Fanconi anemia. *Cell Stem Cell*. 2016;18(5):668-681.
50. Li NS, Zou JR, Lin H, et al. LKB1/AMPK inhibits TGF-β1 production and the TGF-β signaling pathway in breast cancer cells. *Tumour Biol*. 2016;37(6):8249-8258.
51. Algire C, Moiseeva O, Deschênes-Simard X, et al. Metformin reduces endogenous reactive oxygen species and associated DNA damage. *Cancer Prev Res (Phila)*. 2012;5(4):536-543.
52. Batandier C, Guigas B, Detaille D, et al. The ROS production induced by a reverse-electron flux at respiratory-chain complex 1 is hampered by metformin. *J Bioenerg Biomembr*. 2006;38(1): 33-42.
53. Liu X, Zheng H, Yu WM, Cooper TM, Bunting KD, Qu CK. Maintenance of mouse hematopoietic stem cells ex vivo by reprogramming cellular metabolism. *Blood*. 2015;125(10):1562-1565.
54. Nath N, Khan M, Paintlia MK, Singh I, Hoda MN, Giri S. Metformin attenuated the autoimmune disease of the central nervous system in animal models of multiple sclerosis [published correction appears in *J Immunol*. 2009;183(5):3551]. *J Immunol*. 2009;182(12):8005-8014.
55. Li J, Sejas DP, Zhang X, et al. TNF-alpha induces leukemic clonal evolution ex vivo in Fanconi anemia group C murine stem cells. *J Clin Invest*. 2007;117(11):3283-3295.
56. Novelle MG, Ali A, Diéguez C, Bernier M, de Cabo R. Metformin: a hopeful promise in aging research. *Cold Spring Harb Perspect Med*. 2016; 6(3):a025932.

2016 128: 2774-2784
doi:10.1182/blood-2015-11-683490 originally published online October 18, 2016

Metformin improves defective hematopoiesis and delays tumor formation in Fanconi anemia mice

Qing-Shuo Zhang, Weiliang Tang, Matthew Deater, Ngoc Phan, Andrea N. Marcogliese, Hui Li, Muhsen Al-Dhalimy, Angela Major, Susan Olson, Raymond J. Monnat Jr and Markus Grompe

Blood (print ISSN 0006-4971, online ISSN 1528-0020), is published weekly by the American Society of Hematology, 2021 L St, NW, Suite 900, Washington DC 20036.

Cancer Research

Measurement of Endogenous versus Exogenous Formaldehyde–Induced DNA–Protein Crosslinks in Animal Tissues by Stable Isotope Labeling and Ultrasensitive Mass Spectrometry

Yongquan Lai[1], Rui Yu[1], Hadley J. Hartwell[1], Benjamin C. Moeller[2], Wanda M. Bodnar[1], and James A. Swenberg[1]

Abstract

DNA–protein crosslinks (DPC) arise from a wide range of endogenous and exogenous chemicals, such as chemotherapeutic drugs and formaldehyde. Importantly, recent identification of aldehydes as endogenous genotoxins in Fanconi anemia has provided new insight into disease causation. Because of their bulky nature, DPCs pose severe threats to genome stability, but previous methods to measure formaldehyde-induced DPCs were incapable of discriminating between endogenous and exogenous sources of chemical. In this study, we developed methods that provide accurate and distinct measurements of both exogenous and endogenous DPCs in a structurally specific manner. We exposed experimental animals to stable isotope–labeled formaldehyde ([$^{13}CD_2$]-formaldehyde) by inhalation and performed ultrasensitive mass spectrometry to measure endogenous (unlabeled) and exogenous ($^{13}CD_2$-labeled) DPCs. We found that exogenous DPCs readily accumulated in nasal respiratory tissues but were absent in tissues distant to the site of contact. This observation, together with the finding that endogenous formaldehyde–induced DPCs were present in all tissues examined, suggests that endogenous DPCs may be responsible for increased risks of bone marrow toxicity and leukemia. Furthermore, the slow rate of DPC repair provided evidence for the persistence of DPCs. In conclusion, our method for measuring endogenous and exogenous DPCs presents a new perspective for the potential health risks inflicted by endogenous formaldehyde and may inform improved disease prevention and treatment strategies. *Cancer Res; 76(9); 2652–61. ©2016 AACR.*

Introduction

DNA damage is a major culprit in many diseases, including cancer and aging. Toxic chemicals originating from a wide range of endogenous and exogenous sources continuously damage DNA (1). It is well known that our DNA is not pristine, and endogenous DNA damage occurs at a high frequency compared with exogenous damage, having more than 40,000 lesions in every cell in our body (2). The "endogenous exposome" was first explored by our laboratory from the concept of the "exposome" that emphasized the importance of understanding relationships between human disease and lifetime exposures to both environmental and internal chemicals (2). Recent advances have identified endogenous aldehydes as possible genotoxic agents that cause severe bone marrow failure (BMF) and leukemia in mice with mutations in both Fanconi anemia group D2 (*fancd2)* and aldehyde dehydrogenase 2 (*Aldh2*; ref. 3). Notably, *Aldh2* is mutated in approximately 1 billion people, most frequently observed in Southeast Asians due to inherited genetic mutations (4). Deficiency of *Aldh2* has been demonstrated to dramatically accelerate BMF in Japanese Fanconi anemia patients (5). In addition, endogenous formaldehyde has been shown to have greater genotoxicity than acetaldehyde (6–8). These findings raise new challenges for understanding the cellular environments involved in disease causation. Linear extrapolation of risk down to zero remains a common approach used by regulators, despite the fact that such models use no biology and that when biology exists, linear extrapolation will overestimate risks (9). Thus, better understanding of endogenous and exogenous DNA–protein crosslinks (DPC) data is important for advancing science-based risk assessments.

DPCs strongly disrupt normal DNA–protein interactions and interfere with DNA replication, transcription, and repair, which ultimately threatens genomic integrity and cell viability (10). DPCs can originate from exposure to environmental agents, such as ionizing radiation, UV light, formaldehyde, and transition metal ions (11). Furthermore, anticancer drugs have been developed on the basis of their ability to form DPCs, such as nitrogen mustards, platinum-containing agents (i.e., cisplatin), and 5-aza-2′-deoxycytidine. Notably, DPCs can also arise upon exposure to endogenous carcinogens, such as reactive aldehydes that are produced during various cellular processes (2, 12). Because of their bulky nature, DPCs impact practically all aspects of genomic activity and may therefore result in genomic instability or cell

[1]Department of Environmental Sciences and Engineering, Gillings School of Global Public Health, the University of North Carolina at Chapel Hill, Chapel Hill, North Carolina. [2]Lovelace Respiratory Research Institute, Albuquerque, New Mexico.

Note: Supplementary data for this article are available at Cancer Research Online (http://cancerres.aacrjournals.org/).

Corresponding Author: James A. Swenberg, University of North Carolina at Chapel Hill, CB 7431, Chapel Hill, NC 27599. Phone: 919-966-6139; Fax: 919-966-6123; E-mail: jswenber@email.unc.edu

doi: 10.1158/0008-5472.CAN-15-2527

death. Thus, DPC formation and repair are crucial for genomic integrity in humans and consequently for understanding and preventing carcinogenesis (1, 10, 13–15). Surprisingly, however, DPC repair mechanisms have not been fully elucidated (15).

Until now, accurate and distinct measurements of both endogenous and exogenous DPCs have not been studied, which significantly limits our understanding of the biologic effects and repair of DPCs. Accurate measurement of DPCs is complicated by two critical issues. First, covalent DPCs must be completely isolated from non-covalent DNA–protein complexes, as the latter are present in a clear excess over the former throughout the genome (16). Second, DPCs need to be measured with structural specificity, given that there are numerous lesions that complicate the background of DPCs resulting from both endogenous and exogenous electrophiles. However, such stringent measurements of DPCs have not been possible using previously available DPC detection techniques, such as SDS/KCl precipitation, phenol–chloroform extraction, nitrocellulose filter binding, comet assay, alkaline elution, and CsCl density gradient centrifugation, all of which are nonselective (16, 17). Recently, mass spectrometry (MS)–based methods have emerged as powerful tools for chemical analysis of digested DPCs (11). Elegant work using MS has comprehensively characterized and ultrasensitively quantified the DPCs induced by bifunctional electrophiles, such as nitrogen mustards (18, 19), cisplatin, and diepoxybutane (20).

Formaldehyde is classified as an animal and human carcinogen. Humans are exposed to formaldehyde originating from environmental sources due to its broad range of applications and formation from various chemical processes, as well as internal sources due to its role as an essential intermediate of various cellular processes (21). As a strong electrophile, formaldehyde is a well-known crosslinking agent that is cytotoxic, resulting in increased cell proliferation, mutagenesis, and nasal carcinomas in rats exposed by inhalation (22). Formaldehyde has been widely used to elucidate the cellular pathways of DPC repair (8, 10, 23, 24). Furthermore, endogenous formaldehyde is an important source of DNA damage (6, 8). It thus poses unique challenges for understanding the risks associated with exposure. One major question that must be addressed is whether inhaled formaldehyde can increase the risk for leukemia. A critical dilemma has been to determine whether exogenous formaldehyde reaches bone marrow. To this end, we focused on the tissue distribution of endogenous and exogenous formaldehyde–induced DPC formation in rats and nonhuman primates (NHP) at exposure concentrations that had been studied in earlier DPC experiments, as well as in carcinogenicity studies in rats (25–27). For the first time, the incorporation of stable isotope–labeled formaldehyde ([$^{13}CD_2$]-formaldehyde) in animal exposures permitted readily distinguishable measurements of endogenous and exogenous DPCs based on their mass differences through the use of ultrasensitive and selective LC/MS. These measurements of endogenous and exogenous DPCs provide critical new data that advance science-based risk assessment, as well as providing improved methods for understanding pathways for DPC repair, such as the Fanconi anemia pathways, that may lead to better disease treatment.

Materials and Methods

Chemicals and materials

2′-Deoxyguanosine, reduced L-glutathione (GSH), sodium phosphate monobasic (BioXtra), sodium phosphate dibasic (BioXtra), magnesium chloride solution ($MgCl_2$; 1 mol/L), calcium chloride solution ($CaCl_2$; 1 mol/L), sucrose, ammonium acetate, acetic acid, formic acid, formaldehyde–2,4-dinitrophenylhydrazine (DNPH) standards, sodium cyanoborohydride ($NaCNBH_3$), pronase, leucine aminopeptidase M, carboxypeptidase Y, prolidase, alkaline phosphatase, and phosphodiesterase were all purchased from Sigma. DNAzol and Turbo DNase were obtained from Life Technologies. Methanol, acetonitrile, high-performance liquid chromatography (HPLC) grade water, and formaldehyde solution (37%, w/w) were all purchased from Thermo Fisher Scientific. Formaldehyde solution was used to synthesize the dG-Me-Cys standard. [$^{15}N_5$, $^{13}C_{10}$]-deoxyguanosine, [$^{15}N_5$]-deoxyguanosine, [$^{13}CD_2$]-paraformaldehyde (≥98% purity), and [$^{13}CD_2$]-formaldehyde solution (20% w/w in D_2O) were ordered from Cambridge Isotope Laboratories, Inc. [$^{15}N_5$]-deoxyguanosine and [$^{13}CD_2$]-formaldehyde solution were used to synthesize the [$^{15}N_5$]-dG-[$^{13}CD_2$]-Me-Cys (internal standard). DNPH cartridges were ordered from Waters. Proteinase K (20 mg/mL) was obtained from 5 PRIME, Inc. Amicon Ultra Centrifugal Filters (0.5 mL, 3K) were purchased from EMD Millipore. Nanosep Centrifugal Devices (MWCO 3K) were purchased from Pall Life Sciences.

Synthesis of dG-Me-Cys standard and internal standard

A synthesized standard, dG-Me-Cys, was prepared by digestion of dG-Me-GSH according to our previous study (28), using the experimental details described in the Supplementary Information. As demonstrated in a previous study, dG-Me-Cys showed a very close UV absorbance spectrum to that of dG (28). Thus, quantification of dG-Me-Cys was based on a dG standard calibration curve created using a HPLC–UV method with a detection wavelength at 254 nm. For the preparation of internal standard, [$^{15}N_5$]-deoxyguanosine and [$^{13}CD_2$]-formaldehyde were used to synthesize [$^{15}N_5$]-dG-[$^{13}CD_2$]-Me-GSH. Specifically, GSH (100 mmol/L) was incubated with [$^{13}CD_2$]-formaldehyde (60 mmol/L) in 1.0 mL sodium phosphate buffer (100 mmol/L, pH 7.2) at 37°C for 3 hours. [$^{15}N_5$]-dG was then added at a final concentration of 5 mmol/L, and the crosslinking reaction was performed at 37°C for 14 hours. The same methods described in our previous study were applied for the purification and digestion of [$^{15}N_5$]-dG-[$^{13}CD_2$]-Me-Glutathione (28). The isolated [$^{15}N_5$]-dG-[$^{13}CD_2$]-Me-GSH was digested in 0.4 mL sodium phosphate buffer (40 mmol/L, pH 6.0) by carboxypeptidase Y (50 μg/mL) and leucine aminopeptidase M (250 μg/mL) in the presence of $MgCl_2$ (10 mmol/L) and $CaCl_2$ (10 mmol/L) at room temperature for 15 hours. The internal standard, [$^{15}N_5$]-dG-[$^{13}CD_2$]-Me-Cys, was purified and quantified by the same method as described in the Supplementary Information.

DNA-protein crosslink isolation and digestion

Animal exposure was described in the Supplementary Information. DPCs were isolated from animal tissue samples using DNAzol from Life Technologies following the manufacturer's instructions with some modifications. First, animal tissues (30–50 mg) were homogenized in 1 mL of sucrose buffer (20 mmol/L sodium phosphate; 250 mmol/L sucrose, pH 7.2). The nuclei were isolated from homogenate solution by centrifugation at 1,500 × *g* and 4°C for 10 minutes. The nuclear pellets were washed with 1 mL of 20 mmol/L sodium phosphate buffer (pH 7.2). The washed nuclear pellets were dissolved in 50 μL of water, followed by the addition of 800 μL of DNAzol and 20 μL of

proteinase K (20 mg/mL). After protein digestion at room temperature for 15 hours, DPCs were precipitated by adding 600 μL of 100% ethanol. The precipitated DPCs were washed with 800 μL of 75% ethanol 4 times. The isolated DPCs were dissolved in 450 μL digestion buffer (20 mmol/L ammonium acetate, pH 6.0) containing $MgCl_2$ (5 mmol/L), $CaCl_2$ (5 mmol/L), DNase I (40 U/mL), alkaline phosphatase (4 U/mL), phosphodiesterase I (0.001 U/mL), and pronase (0.5 mg/mL). DNA digestion was performed at room temperature for 20 hours, resulting in the formation of nucleoside–peptide crosslinks. The enzymes and undigested DNA were removed using a Nanosep Centrifugal Device (MWCO, 3K) at 10,000 × *g* and 4°C for 40 minutes. The resultant filtrate was combined with 30 μL of an enzyme mixture containing carboxypeptidase Y (0.3 mg/mL), aminopeptidase M (0.6 mg/mL), and prolidase (0.3 mg/mL) to further digest peptides to amino acids. Following a 20-hour incubation at room temperature, the reaction was terminated with the addition of 4 μL of 30% acetic acid. After adding 8 fmol of internal standard (4 μL, 2 nmol/L), the final reaction mixtures were subjected to centrifugation at 10,000 × *g* and 4°C for 40 minutes in a Nanosep Centrifugal Device to remove enzymes prior to HPLC purification. To eliminate matrix interferences, digestion enzymes were washed before use as described in the Supplementary Information.

HPLC purification and fractionation

The target analyte, dG-Me-Cys, was purified from the reaction mixture on an Agilent 1200 Series UV HPLC System by using two C_{18} reverse-phase columns connected in series (Waters Atlantis T3, 3 μm, 150 mm × 4.6 mm). Following digestion, there were two products detected by HPLC–UV, both of which had similar retention times to that of DPCs. The use of two HPLC columns connected in series was found to greatly increase the resolution of HPLC separation between the dG-Me-Cys and the other digestion products. This increased the detection sensitivity of the DPC using nano-LC/ESI/MS-MS. The detection wavelength and column temperature were set at 254 nm and 15°C, respectively. The mobile phases consisted of 0.05% acetic acid in water (A) and pure acetonitrile (B). The flow rate was 0.45 mL/minute, and elution gradient conditions were set as follows: 0 minute, 1% B; 3 minutes, 1% B; 42 minutes, 3% B; 86 minutes, 3.5% B; 86.5 minutes, 80% B; 95 minutes, 80% B; 95.5 minutes, 1% B; 110 minutes, 1% B. dG-Me-Cys was eluted at a retention time of 81.5 minutes. The fractions containing target compounds were combined and concentrated to approximately 10 to 20 μL using a vacuum concentrator. The amount of digested dG in each sample was quantitated by the UV peak area (λ = 254 nm) at the corresponding retention time using a calibration curve ranging from 4 to 80 nmole dG on column.

Nano-LC/ESI/MS-MS analysis

Nano-LC/ESI/MS-MS analysis of dG-Me-Cys was performed on a TSQ Quantum Ultra Triple-Stage Quadrupole Mass Spectrometer (Thermo Scientific) in positive-mode electrospray ionization. Selected reaction monitoring (SRM) mode was used to detect and quantify dG-Me-Cys. Sample introduction and separation was accomplished on a nanoACQUITY Ultra Performance Liquid Chromatography system from Waters Corporation. Following injection, the compounds were retained on two Symmetry C_{18} trap columns (5 μm, 20 × 0.18 mm) connected in series, followed by sample separation on a HSS T3 analytical column (1.8 μm, 100 × 0.1 mm) from Waters Corporation at room temperature. Mobile phases consisted of water with 0.05% acetic acid (A) and acetonitrile (B). Analytes were first retained on two trap columns with a flow rate of 1.8 μL/minute of 1% mobile phase B for 3 minutes, followed by transfer to the analytical column. The flow rate was 0.4 μL/minute, and elution gradient conditions were set as follows: 0 minute, 1% B; 3 minutes, 1% B; 16 minutes, 50% B; 20 minutes, 1% B; 35 minutes, 1% B. Mass spectrometer conditions were set as the following: source voltage, 2,200 V; temperature of ion transfer tube, 280°C; skimmer offset, 0; scan speed, 75 ms; scan width, 0.7 *m/z*; Q1 and Q3 peak width, 0.7 *m/z*; collision energy, 31 eV; collision gas (argon), 1.5 arbitrary units. A sample volume of 5 μL was injected for analysis. Endogenous DPC (dG-Me-Cys) and exogenous DPC (dG-[$^{13}CD_2$]-Me-Cys) were quantified by using the transition of *m/z* 401.1 to *m/z* 164.1 and *m/z* 404.1 to *m/z* 167.1, respectively. The transition of *m/z* 409.1 to *m/z* 172.1 was monitored for the internal standard ([$^{15}N_5$]-dG-[$^{13}CD_2$]-Me-Cys). Linear calibration curves were obtained using the ratio of integrated peak area of the analytic standard over that of the internal standard.

Method validation for LC/ESI/MS-MS analysis

Standard curves were established by plotting the peak area ratios of solutions containing a fixed amount of internal standard ([$^{15}N_5$]-dG-[$^{13}CD_2$]-Me-Cys, 8.0 fmol) and increasing amounts of dG-Me-Cys from 0.15 to 6 fmol. The limit of quantification was determined as the amount of standard that produced a signal-to-noise ratio >10. To evaluate method accuracy and precision, analytic standard was spiked into the digested mixture of rat liver samples at three different levels (0.8, 2.0, and 5.0 fmol), followed by HPLC purification and concentration using a vacuum concentrator.

Artifact determination

The digestion process of DPCs isolated from animal tissues has the potential to generate some chemically reactive species, including nucleotides containing a hydroxymethyl group, hydroxymethyl-dG, dG, and peptides containing cysteine. These products could potentially crosslink to form artifactual dG-Me-Cys during sample preparation. Control studies were performed to determine the potential for artifactual formation of dG-Me-Cys. The extent of possible artifacts was evaluated in two ways. The first technique involved spiking isotope–labeled [$^{13}C_{10}$, $^{15}N_5$]-dG into the DPC solution to determine the potential for extrinsic formation of [$^{13}C_{10}$, $^{15}N_5$]-dG-Me-Cys. Specifically, [$^{13}C_{10}$, $^{15}N_5$]-deoxyguanosine (4 mmol/L) was treated with 600 μL of 0.5 mol/L $NaCNBH_3$ for 48 hours at 37°C. The treated [$^{13}C_{10}$, $^{15}N_5$]-dG was spiked into an equal amount of dG produced from DNA digestion. This spiked sample was subjected to DNA and protein digestion, followed by HPLC purification and LC/ESI/MS-MS analysis as described above. The potential artifact, [$^{13}C_{10}$, $^{15}N_5$]-dG-Me-Cys, was monitored using the corresponding transition of *m/z* 416.1 to *m/z* 174.1. The second technique to determine artifact formation employed $NaCNBH_3$ to reduce active hydroxymethyl groups in DNA and protein during the isolation of DPCs. Specifically, all solutions used in the isolation of DPCs, including homogenate buffer, wash solution, and DNazol, contained 20 mmol/L $NaCNBH_3$. For control samples, $NaCNBH_3$ was excluded in all solutions used for DPC isolation.

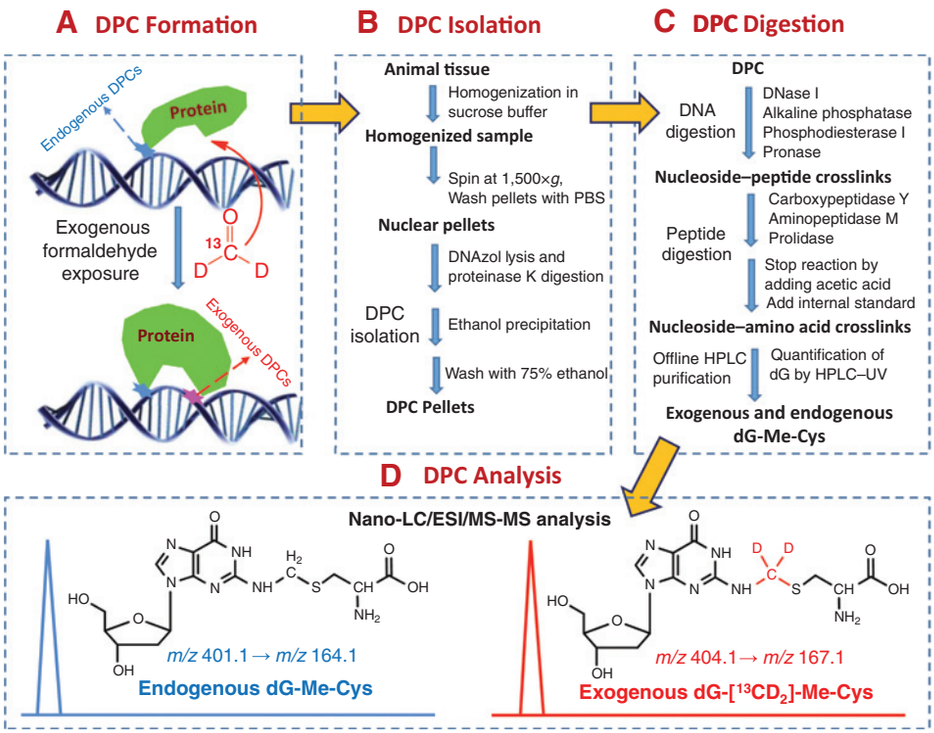

Figure 1.
Experimental workflow for distinct measurement of endogenous and exogenous DPCs. A, animals were exposed to [$^{13}CD_2$]-formaldehyde by inhalation. The use of [$^{13}CD_2$]-formaldehyde allowed the differentiation of endogenous and exogenous dG-Me-Cys crosslinks having the same chemical identity, but different masses. B, DPCs were isolated from animal tissues using a DNAzol method. C, DPCs were digested to nucleoside–amino acid crosslinks by DNA and protein enzymes, followed by offline HPLC purification of formaldehyde DPCs, along with quantification of digested dG. D, endogenous and exogenous formaldehyde DPCs were differentially quantified as the corresponding dG-Me-Cys using nano-LC/MS-MS. The normalization of DPC concentration was achieved by calculating the ratio of the amount of dG-Me-Cys to digested dG.

Results

Isolation and detection of formaldehyde-specific DPCs

To study the chemical identity of formaldehyde-induced DPCs, we investigated the *in vitro* crosslinking reaction between nucleosides and amino acids in the presence of formaldehyde (29). Our results demonstrated that dG and cysteine crosslinked in the presence of formaldehyde to form dG-Me-Cys. We hypothesized that this crosslink would serve as a specific DPC biomarker of formaldehyde exposure based on its relatively high stability and abundance. To test this hypothesis, we examined formaldehyde-induced DPCs, specifically dG-Me-Cys, in both rats and NHPs that were exposed to [$^{13}CD_2$]-formaldehyde using nose-only and whole-body inhalation chambers, respectively (Fig. 1A and Supplementary Figs. S2 and S3). The use of [$^{13}CD_2$]-formaldehyde permitted the differential measurement of endogenous and exogenous dG-Me-Cys based on their mass difference (+3 *m/z*) by MS. A challenging step in structurally specific analysis of DPCs is the digestion or hydrolysis of bulky DPCs into small molecules suitable for MS-MS analysis. Many DPCs are unstable, and chemical hydrolysis is generally too harsh to preserve the DPC linkages for their chemical identities. To this end, we optimized a mixture of enzymes to digest large DPCs into small nucleoside–amino acid crosslinks (dG-Me-Cys) under mild conditions (pH 6.0 and room temperature), thereby enabling preservation of the DPC chemical identity before MS analysis (Fig. 1B and C). After complete digestion, formaldehyde-induced DPCs were isolated by offline HPLC fraction collection along with the quantification of digested dG using UV absorbance at 256 nm. Using authentic standards, the isolated endogenous and exogenous dG-Me-Cys were differentially quantified by MS (Fig. 1D).

Nano UPLC/MS-MS method development for DPC analysis

Given the inherent advantage of improved sensitivity, we adopted a nanospray UPLC/ESI/MS-MS methodology to measure dG-Me-Cys. The validated method exhibits ultrasensitivity, as well as excellent accuracy and precision. Both the standard (dG-Me-Cys) and the internal standard were detected at the same retention time (Fig. 2). The limit of quantification was 37.5 amol on the column (S/N = 10). Good linearity was observed in the concentration range from 0.15 to 6.0 fmol with an R^2 value of 0.9993 (Supplementary Fig. S1). The accuracy of this method was greater than 93.4%, with precision being less than 11.2% RSD using three spiking concentrations: 0.8, 2.0, and 5 fmol (Supplementary Table S1).

The validated method was then utilized to identify endogenous and exogenous formaldehyde–specific DPCs in rat nasal tissue (respiratory epithelium) as shown in Fig. 3. Only the endogenous peak (dG-Me-Cys) corresponding to the specific transition of *m/z* 401.1 to *m/z* 164.1 was detected in control rat nasal tissue at the same retention time as the internal standard at 14.20 minutes (Fig. 3A). Both endogenous and exogenous crosslinks were detected in [$^{13}CD_2$]-formaldehyde–exposed rat nasal tissue at the same chromatographic retention time (Fig. 3B). The exogenous DPC fragment ions retained the stable isotope label, demonstrating the predicted isotope mass shift (+3 *m/z*) and were clearly distinguished from fragment ions of endogenous origin.

Artifact determination for the validated method

The potential for artifactual dG-Me-Cys formation during sample processing was investigated in two ways. First, stable isotope–labeled [$^{13}C_{10}$, $^{15}N_5$]-dG was spiked into the reaction mixture to investigate whether free dG from the DNA digestion could form

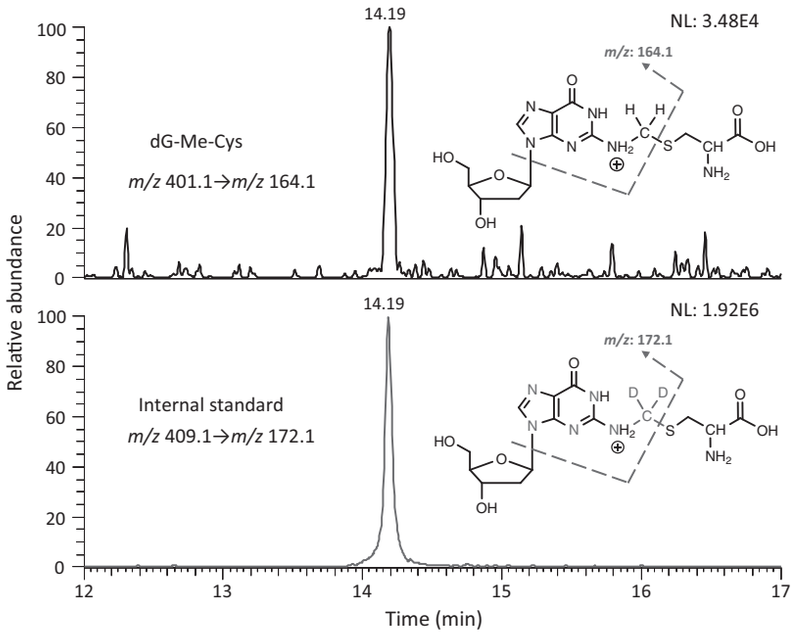

Figure 2.
Typical nano-LC/ESI/MS-MS/SRM chromatogram of dG-Me-Cys. Nano-LC/ESI/MS-MS/SRM chromatograms of dG-Me-Cys (0.0375 fmol) and internal standard [$^{15}N_5$]-dG-[$^{13}CD_2$]-Me-Cys (0.5 fmol). NL, normalized spectrum to largest peak in this particular chromatogram.

the crosslink. The potential formation of artifact, [$^{13}C_{10}$, $^{15}N_5$]-dG-Me-Cys, was monitored using the corresponding transition of *m/z* 416.1 to *m/z* 174.1. The results showed that endogenous dG-Me-Cys and internal standard were observed as shown in the top and middle panels of Fig. 4A, respectively. On the contrary, no peak corresponding to the artifactual formation of [$^{13}C_{10}$, $^{15}N_5$]-dG-Me-Cys was found in the same sample (Fig. 4A, bottom). This evidence demonstrated that the digestion of dG does not lead to artifactual formation of dG-Me-Cys during sample preparation. The second technique employed $NaCNBH_3$ to reduce active hydroxymethyl groups that could possibly form artifactual dG-Me-Cys (Fig. 4B). The results demonstrated that the reduction of hydroxymethyl groups did not change the amount of dG-Me-Cys in rat liver samples. These data imply that the digested dG and other products do not generate artifacts that interfere with the detection of DPCs.

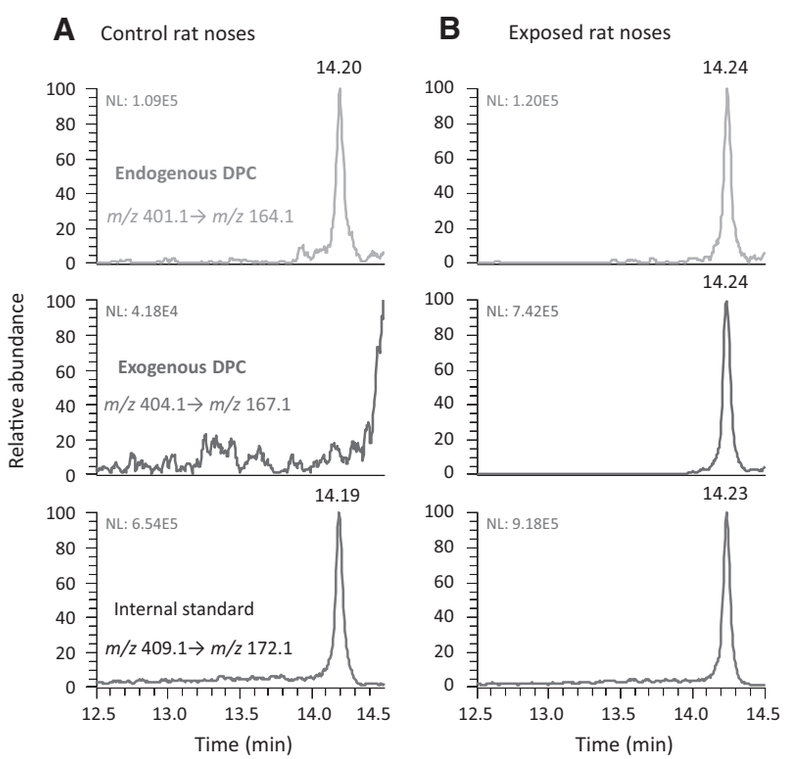

Figure 3.
Distinct detection of endogenous and exogenous dG-Me-Cys in control (A) and exposed rat noses (B) by nano-LC/MS-MS. NL, normalized spectrum to largest peak in this particular chromatogram.

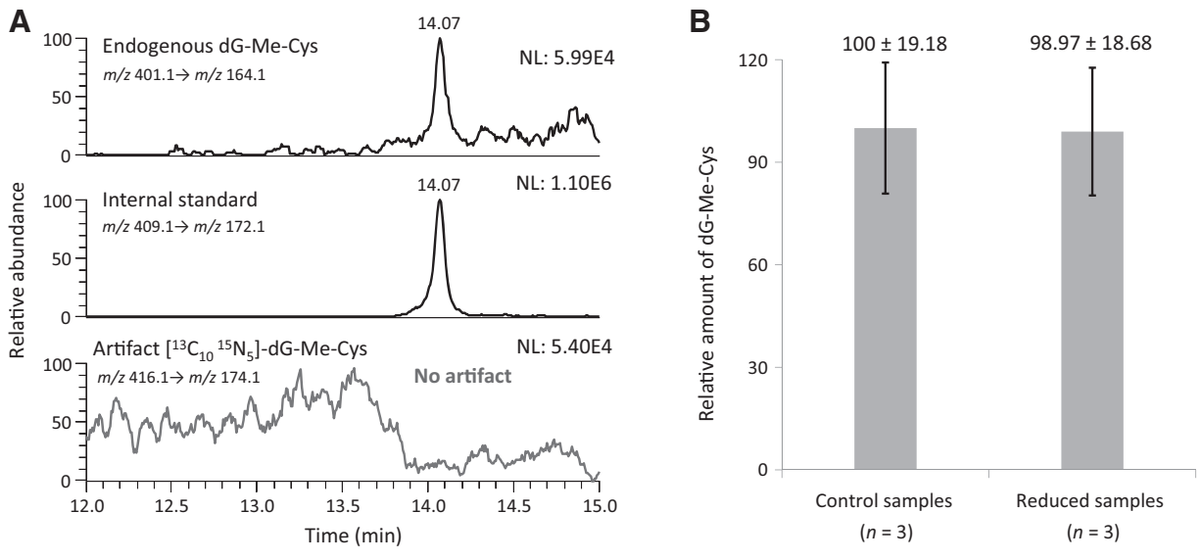

Figure 4.
Evaluation of artifactual formation of dG-Me-Cys. A, artifact determination in a rat liver sample spiked with isotope-labeled [$^{13}C_{10}$, $^{15}N_5$]-dG. B, relative amount of endogenous dG-Me-Cys in rat liver samples treated without (control sample) and with $NaCNBH_3$ (reduced sample). Error bars represent the SD of three individual experiments. NL, normalized spectrum to largest peak in this particular chromatogram.

Distribution of formaldehyde-induced DPCs in rats and monkeys

Using this sensitive method, endogenous and exogenous formaldehyde–induced DPCs were distinctly quantified in selected tissues [nasal epithelium, peripheral blood mononuclear cells (PBMC), bone marrow, and liver] of animals exposed to either filtered air only or [$^{13}CD_2$]-formaldehyde. Consistent results from rat and NHP studies clearly demonstrate that exogenous DPCs were only found in the nasal epithelium of animals exposed to varying amounts of [$^{13}CD_2$]-formaldehyde. Specifically, exogenous DPCs were detected at 1.36 ± 0.20 crosslinks/10^8 dG in NHP nasal tissues exposed to [$^{13}CD_2$]-formaldehyde, with a targeted aerosol concentration of 6.0 ppm for 2 consecutive days (6 hours/day; Table 1). A much higher number of exogenous DPCs were measured at 18.18 ± 7.23 crosslinks/10^8 dG in the rat nasal tissues from animals exposed to [$^{13}CD_2$]-formaldehyde at a targeted concentration of 15 ppm for 4 consecutive days (6 hours/day; Table 2). In contrast to the exogenous DPCs, endogenous DPCs were present in all examined tissues in both air control and exposed animals. Surprisingly, endogenous DPCs were present at higher amounts, compared with exogenous DPCs in exposed NHP nasal tissue (Table 1). More strikingly, the number of endogenous DPCs (15.46 ± 1.98 crosslinks/10^8 dG) in air control NHP livers was close to the highest amounts of exogenous DPCs (18.18 ± 7.23 crosslinks/10^8 dG) observed in the rat nasal tissues exposed to 15 ppm [$^{13}CD_2$]-formaldehyde for 4 consecutive days, a highly carcinogenic exposure concentration in the rat cancer bioassays (30–32).

Formation and elimination of formaldehyde-induced DPCs in rat nasal tissues

To monitor the induction and elimination of DPCs, we applied our method to investigate the accumulation and persistence of formaldehyde-induced DPCs in rat nasal tissues. As shown in Tables 2 and 3, both high and low exposure concentrations of inhaled formaldehyde gave rise to the accumulation of exogenous DPCs in rat nasal tissues. At a high exposure concentration of 15 ppm [$^{13}CD_2$]-formaldehyde, similar amounts of exogenous DPCs were detected in 1-day and 2-day exposed rat nasal tissues (5.52 ± 0.80 and 4.69 ± 1.76 crosslinks/10^8 dG), whereas 4-day exposed rat nasal tissues showed a dramatic increase in the formation of exogenous DPCs (18.18 ± 7.23 crosslinks/10^8

Table 1. Formaldehyde-induced dG-Me-Cys in nose, PBMCs, bone marrow, and liver of primates exposed to air control versus 6 ppm of [$^{13}CD_2$]-formaldehyde (6 h/day)

Tissue	Targeted [$^{13}CD_2$]-formaldehyde concentration (ppm)	Exposure period (days)	dG-Me-Cys (crosslink/10^8 dG)	
			Endogenous	Exogenous
Nose	Air control	2	3.59 ± 1.01 ($n = 5$)	ND
	6 ppm	2	3.76 ± 1.50 ($n = 5$)	1.36 ± 0.20
PBMC	Air control	2	1.34 ± 0.25 ($n = 5$)	ND
	6 ppm	2	1.57 ± 0.58 ($n = 4$)	ND
Bone marrow	Air control	2	2.30 ± 0.30 ($n = 4$)	ND
	6 ppm	2	1.40 ± 0.46 ($n = 5$)	ND
Liver	Air control	2	15.46 ± 1.98 ($n = 6$)	ND
	6 ppm	2	11.80 ± 2.21 ($n = 6$)	ND

Abbreviation: ND, not detected.

Table 2. Formaldehyde-induced dG-Me-Cys in nasal tissue, PBMCs, and bone marrow of rats exposed to air control verses 15 ppm of [$^{13}CD_2$]-formaldehyde (6 h/day)

Tissue	Targeted [$^{13}CD_2$]-formaldehyde concentration (ppm)	Exposure period (days)	dG-Me-Cys (crosslink/10^8 dG)	
			Endogenous	Exogenous
Nasal	Air control	4	6.50 ± 0.30 ($n = 5$)	ND
	15.0	1	4.42 ± 1.10 ($n = 6$)	5.52 ± 0.80
	15.0	2	4.28 ± 2.34 ($n = 6$)	4.69 ± 1.76
	15.0	4	3.67 ± 0.80 ($n = 6$)	18.18 ± 7.23
PBMC	Air control	4	4.98 ± 0.61 ($n = 5$)	ND
	15.0	1	3.26 ± 0.73 ($n = 4$)	ND
	15.0	2	3.00 ± 0.98 ($n = 5$)	ND
	15.0	4	7.19 ± 1.73 ($n = 5$)	ND
Bone marrow	Air control	4	1.64 ± 0.49 ($n = 4$)	ND
	15.0	1	1.80 ± 0.47 ($n = 4$)	ND
	15.0	2	1.84 ± 0.61 ($n = 4$)	ND
	15.0	4	1.58 ± 0.38 ($n = 4$)	ND

Abbreviation: ND, not detected.

dG; Table 2). In contrast to the large changes in exogenous DPC formation, less difference in the amounts of endogenous DPCs were present in the same samples, suggesting that the endogenous DPCs were at steady-state concentrations. Most importantly, exogenous DPCs showed little change in the animals exposed for 28 days with either a 24- or 168-hour (7 days) postexposure recovery period (Table 3), indicating high stability and long-term persistence of DPCs with the dG-Me-Cys linkage. The discovery of accumulation and persistence of formaldehyde-DPCs highlights the need for a better understanding of DPC stability and repair.

Discussion

Formaldehyde was first shown to be an animal carcinogen in 1980, causing squamous cell carcinomas in the nasal passages of exposed rats at concentrations at or above 6 ppm (30, 31). Recent epidemiologic studies have suggested that exposure to formaldehyde vapors may lead to the development of hematopoietic cancers, such as leukemia; however, these findings remain under debate (28, 33–37). Although leukemia has been a major finding in epidemiology studies of inhaled formaldehyde, no mechanism for leukemia has been established. The International Agency for Research on Cancer working group also was not in full agreement on the evaluation of formaldehyde causing leukemia in humans (22, 38). A recent article by Coggon and colleagues did not find any leukemias in one of the largest cohorts of formaldehyde workers, even though some of those workers were exposed to inhaled formaldehyde at concentrations much higher than 2 ppm (37). In addition, the induction of leukemia by inhaled formaldehyde exposures has not been supported in rat carcinogenicity studies (39). Previous studies in rats and NHP also have not found any evidence that inhaled [$^{13}CD_2$]-formaldehyde reached the bone marrow as exogenous DNA adducts (28, 34).

Endogenous formaldehyde is produced as an essential metabolic intermediate by enzymatic and nonenzymatic pathways and as a detoxification product of xenobiotics during cellular metabolism (40). It is well understood that endogenous formaldehyde originates from numerous sources including one-carbon pool metabolism, amino acid metabolism, methanol metabolism, lipid peroxidation, cytochrome P450–catalyzed demethylation, and histone demethylation reactions (34, 41, 42). Endogenous formaldehyde has been assumed to be present in all aqueous body fluids because of its water solubility. Its half-life in humans is estimated to be 1 to 1.5 minutes (43). In particular, the concentration of endogenous formaldehyde was detected at approximately 0.1 mmol/L in the blood of rats, monkeys, and humans (22, 44–46). In addition, endogenous formaldehyde was found to be 2 to 4 times higher in the liver and nasal mucosa than in the blood of a rat (47). Endogenous formaldehyde is also formed in cellular nuclei, secondary to demethylation of histone III (42). These formaldehyde molecules are released in close proximity to DNA, providing an important source for bone marrow DPC and formaldehyde monoadducts (42). Thus, with endogenous formaldehyde–induced DNA adducts and DPC present in all tissues examined, but a complete lack of exogenous DNA adducts and DPC in tissues distant to the portal of entry (6, 28), the key issue that must be addressed by risk assessors and epidemiologists is whether or how exogenous formaldehyde exposure could increase cancer risks at distal sites.

Because of their significant biologic consequences, formaldehyde-induced DPCs have long been recognized as a highly mutagenic form of formaldehyde DNA damage. The amounts of formaldehyde-induced DPCs are considered to represent a good molecular biomarker of formaldehyde exposure (6, 48). However, the lack of robust DPC measurements has limited our understanding of the genotoxic activity of formaldehyde. Previous studies using chloroform/isoamyl alcohol/phenol extraction–based DPC isolation following inhaled formaldehyde exposures in rats and NHPs found increased amounts of DPC formation in the nasal tissue, but not in tissues distant from the portal of entry (25, 27). In contrast, increased numbers of DPCs were detected in circulating lymphocytes of workers occupationally exposed to formaldehyde and in remote tissues, such as bone marrow, liver, kidney, and testes of mice exposed to inhaled formaldehyde using SDS/KCl precipitation–based DPC isolation (49, 50). This scientific dispute may be due to the major disadvantage of previous DPC assays that were unable to provide chemical identity for specific and accurate measurements of DPCs. Furthermore, it is has been impossible to distinguish endogenous from

Table 3. Formaldehyde-induced dG-Me-Cys in nose of rats exposed to 2 ppm of [$^{13}CD_2$]-formaldehyde (6 h/day) for up to 28 days

Exposure period (day)	dG-Me-Cys (crosslink/10^8 dG)	
	Endogenous	Exogenous
7 days	4.78 ± 0.64 ($n = 4$)	0.96 ± 0.17
28 days	4.51 ± 1.48 ($n = 3$)	2.46 ± 0.44
28 days + 24 h post exposure	3.78 ± 0.69 ($n = 4$)	2.12 ± 1.00
28 days + 168 h post exposure	3.51 ± 0.16 ($n = 3$)	2.14 ± 1.02

exogenous formaldehyde–induced DPCs prior to the use of stable isotopes.

In particular, the National Research Council (NRC) committee considered our earlier work using sensitive and distinct measurements between exogenous and endogenous formaldehyde–induced DNA adducts as being highly informative and should be incorporated in the U.S. Environmental Protection Agency (EPA) draft Integrated Risk Information System (IRIS) assessment (34, 48). Moreover, the NRC committee suggested that DPCs play a more important role in formaldehyde genotoxicity and carcinogenicity compared with DNA adducts (48). This study provides accurate measurements that discriminate between endogenous and exogenous DPCs through the use of stable isotope formaldehyde exposures and ultrasensitive MS. Our data demonstrate that exogenous DPCs were only found in nasal samples of exposed animals, but not in sites remote to the portal of entry. Consistently, our previous studies reported that inhaled formaldehyde–induced DNA adducts and protein adducts were only detected in rat and NHP nasal tissues, but not in other tissues, such as lung, liver, bone marrow, and PBMC (28, 34, 51). These findings suggest that there is no additional dose to the bone marrow beyond that from endogenous formaldehyde. The lack of exogenous DPCs in remote tissues does not support a plausible relationship between inhaled formaldehyde and increased risks of leukemia. On the other hand, with high amounts of endogenous formaldehyde always present in all cells, one would expect the induction of disease states by this highly reactive aldehyde. Our previous work identified specific DNA adducts (N^2-Me-dG) and DNA–DNA crosslinks (dG-Me-dG) induced by endogenous formaldehyde (34). This study provides the first evidence to the existence of endogenous formaldehyde–induced DPCs in all examined tissues. Furthermore, the recent article by our laboratory and Pontel and colleagues clearly demonstrated that endogenous formaldehyde is a hematopoietic genotoxin and a metabolic carcinogen (6). In addition, as recently reported, as many as 1 of 3 acute myeloid leukemia patients have deficiencies in aldehyde dehydrogenases that play important roles in preventing DNA damage by detoxifying endogenous aldehydes (52). Thus, recent medical research has provided strong data that better explain the formaldehyde epidemiology findings.

Formaldehyde-induced DPCs had been considered to be unstable in cell and animal studies. A rapid decline of the formaldehyde-induced DPCs was reported in cell culture, and there was no accumulation of DPCs observed in rat nasal tissues after repeated exposure (16, 53, 54). However, this study demonstrated that exogenous DPCs accumulated with exposure time and showed little change after one week postexposure. Previous inconsistent results may be due to the use of nonstructurally specific measurements, which are highly susceptible to the interference of non-covalent DNA protein complexes. Although DPC repair mechanisms have not been well understood, proteolysis of the protein components of the DPC to small peptides has been reported as a protease-based DNA repair pathway specific for DPCs (10, 11, 15, 55). This study measures single amino acid–nucleoside crosslinks, specifically dG-Me-Cys. The small change in the amount of dG-Me-Cys measured one week postexposure does not rule out the possibility that the protein components of DPCs as a whole do not undergo proteolytic degradation to small peptides. In a recent study, synthesized DPCs, including dG-Me-cysteine, dG-Me-GSH, and dG-Me-peptide crosslinks, were found to undergo rapid hydrolysis *in vitro* (28). The long-term persistence of DPCs observed *in vivo* is likely due to the steric hindrance and localized hydrophobic conditions of DNA and the associated protein that greatly increase DPC stability.

The success of distinctly measuring endogenous and exogenous formaldehyde DPCs has demonstrated the importance of structurally specific DPC data. The lack of exogenous DPCs in remote tissues away from the portal of entry suggests that the effects of inhaled formaldehyde may have been overemphasized, while endogenous formaldehyde has been underappreciated as a source of exposure leading to the induction of leukemia. The finding of exogenous DPC accumulation during inhalation exposure and its minimal repair following one week postexposure provides the first evidence of long-term persistence of DPCs. The discovery of endogenous DPCs in all tissues examined raises an important perspective on the potential health risks posed by endogenous formaldehyde. Considering the high background of endogenous DPCs, it would be impossible to measure the induction, distribution, and elimination of exogenous DPCs without exogenous DPC measurements, particularly at low levels of exposure.

Future applications of this method include, but are not limited to, (i) investigation of DPC repair mechanism(s) *in vivo* using formaldehyde-induced DPCs; (ii) understanding whether and how the Fanconi anemia genes are involved in aldehyde-induced DPC repair; (iii) application of such data for science-based risk assessment of aldehydes in a manner that contributes to the EPA's IRIS program assessment of formaldehyde and aldehydes in general; (iv) utilizing structurally specific methodologies to determine the makeup of DPCs induced by various endogenous and exogenous agents, such as malondialdehyde, 4-hydroxynonenal, acrolein, and aldehydic lesions present on abasic sites. Likewise, DPCs associated with exogenous anticancer drugs can be understood better, contributing to further advancements of chemotherapy. In summary, this study provides a new approach to accurately determine the roles of endogenous and environmental DPCs to form mutagenic DNA damage as factors that contribute to disease and provide more accurate data that can improve cancer risk assessments.

Disclosure of Potential Conflicts of Interest

No potential conflicts of interest were disclosed.

Authors' Contributions

Conception and design: Y. Lai, R. Yu, B.C. Moeller, J.A. Swenberg
Development of methodology: Y. Lai, H.J. Hartwell, B.C. Moeller
Acquisition of data (provided animals, acquired and managed patients, provided facilities, etc.): Y. Lai, H.J. Hartwell, B.C. Moeller, W.M. Bodnar, J.A. Swenberg
Analysis and interpretation of data (e.g., statistical analysis, biostatistics, computational analysis): Y. Lai, R. Yu, H.J. Hartwell, B.C. Moeller, J.A. Swenberg
Writing, review, and/or revision of the manuscript: Y. Lai, R. Yu, H.J. Hartwell, B.C. Moeller, W.M. Bodnar, J.A. Swenberg
Administrative, technical, or material support (i.e., reporting or organizing data, constructing databases): Y. Lai, H.J. Hartwell, B.C. Moeller, J.A. Swenberg
Study supervision: B.C. Moeller, J.A. Swenberg

Acknowledgments

The authors thank Dean Kracko, Raul Romero, and Dr. Melanie Doyle-Eisele at Lovelace Respiratory Research Institute for providing technical assistance and guidance in setting up and conducting the animal exposures. The costs of animal exposures at Lovelace Respiratory Research Institute were generously provided

by Formacare and the Research Foundation for Health and Environmental Effects. The authors also thank Leonard B. Collins for his assistance with HPLC purification and nano-UPLC-MS-MS.

Grant Support

This work was supported by the National Institutes of Environmental Health Sciences (NIEHS) Superfund Basic Research Program (P42 ES005948), NIEHS Center for Environmental Health and Susceptibility (P30 ES010126), the Texas Commission for Environmental Quality (582-12-21861), and Formacare.

The costs of publication of this article were defrayed in part by the payment of page charges. This article must therefore be hereby marked *advertisement* in accordance with 18 U.S.C. Section 1734 solely to indicate this fact.

Received September 9, 2015; revised January 26, 2016; accepted February 14, 2016; published OnlineFirst March 16, 2016.

References

1. Sczepanski JT, Wong RS, McKnight JN, Bowman GD, Greenberg MM. Rapid DNA-protein cross-linking and strand scission by an abasic site in a nucleosome core particle. Proc Natl Acad Sci U S A 2010;107:22475–80.
2. Nakamura J, Mutlu E, Sharma V, Collins L, Bodnar W, Yu R, et al. The endogenous exposome. DNA Repair 2014;19:3–13.
3. Garaycoechea JI, Crossan GP, Langevin F, Daly M, Arends MJ, Patel KJ. Genotoxic consequences of endogenous aldehydes on mouse haematopoietic stem cell function. Nature 2012;489:571–5.
4. Perez-Miller S, Younus H, Vanam R, Chen CH, Mochly-Rosen D, Hurley TD. Alda-1 is an agonist and chemical chaperone for the common human aldehyde dehydrogenase 2 variant. Nat Struct Mol Biol 2010;17:159–64.
5. Hira A, Yabe H, Yoshida K, Okuno Y, Shiraishi Y, Chiba K, et al. Variant ALDH2 is associated with accelerated progression of bone marrow failure in Japanese Fanconi anemia patients. Blood 2013;122:3206–9.
6. Pontel Lucas B, Rosado Ivan V, Burgos-Barragan G, Garaycoechea Juan I, Yu R, Arends Mark J, et al. Endogenous formaldehyde is a hematopoietic stem cell genotoxin and metabolic carcinogen. Mol Cell 2015;60:177–88.
7. Duxin JP, Walter JC. What is the DNA repair defect underlying Fanconi anemia? Curr Opin Cell Biol 2015;37:49–60.
8. Rosado IV, Langevin F, Crossan GP, Takata M, Patel KJ. Formaldehyde catabolism is essential in cells deficient for the Fanconi anemia DNA-repair pathway. Nat Struct Mol Biol 2011;18:1432–4.
9. Crump KS. The linearized multistage model and the future of quantitative risk assessment. Hum Exp Toxicol 1996;15:787–98.
10. Stingele J, Schwarz MS, Bloemeke N, Wolf PG, Jentsch S. A DNA-dependent protease involved in DNA-protein crosslink repair. Cell 2014;158:327–38.
11. Tretyakova NY, Groehler A, Ji S. DNA–protein cross-links: formation, structural identities, and biological outcomes. Acc Chem Res 2015;48:1631–44.
12. Voulgaridou GP, Anestopoulos I, Franco R, Panayiotidis MI, Pappa A. DNA damage induced by endogenous aldehydes: current state of knowledge. Mutat Res 2011;711:13–27.
13. Reardon JT, Sancar A. Repair of DNA-polypeptide crosslinks by human excision nuclease. Proc Natl Acad Sci U S A 2006;103:4056–61.
14. Nakano T, Morishita S, Katafuchi A, Matsubara M, Horikawa Y, Terato H, et al. Nucleotide excision repair and homologous recombination systems commit differentially to the repair of DNA-protein crosslinks. Mol Cell 2007;28:147–58.
15. Duxin JP, Dewar JM, Yardimci H, Walter JC. Repair of a DNA-protein crosslink by replication-coupled proteolysis. Cell 2014;159:346–57.
16. Shoulkamy MI, Nakano T, Ohshima M, Hirayama R, Uzawa A, Furusawa Y, et al. Detection of DNA-protein crosslinks (DPCs) by novel direct fluorescence labeling methods: distinct stabilities of aldehyde and radiation-induced DPCs. Nucleic Acids Res 2012;40:e143.
17. Ide H, Shoulkamy MI, Nakano T, Miyamoto-Matsubara M, Salem AM. Repair and biochemical effects of DNA-protein crosslinks. Mutat Res 2011;711:113–22.
18. Loeber R, Michaelson E, Fang Q, Campbell C, Pegg AE, Tretyakova N. Cross-linking of the DNA repair protein Omicron6-alkylguanine DNA alkyltransferase to DNA in the presence of antitumor nitrogen mustards. Chem Res Toxicol 2008;21:787–95.
19. Michaelson-Richie ED, Ming X, Codreanu SG, Loeber RL, Liebler DC, Campbell C, et al. Mechlorethamine-induced DNA-protein cross-linking in human fibrosarcoma (HT1080) cells. J Proteome Res 2011;10:2785–96.
20. Gherezghiher TB, Ming X, Villalta PW, Campbell C, Tretyakova NY. 1,2,3,4-Diepoxybutane-induced DNA-protein cross-linking in human fibrosarcoma (HT1080) cells. J Proteome Res 2013;12:2151–64.
21. Swenberg JA, Lu K, Moeller BC, Gao L, Upton PB, Nakamura J, et al. Endogenous versus exogenous DNA adducts: their role in carcinogenesis, epidemiology, and risk assessment. Toxicol Sci 2011;120 Suppl 1:S130–S145.
22. IARC. Formaldehyde, 2-Butoxyethanol and 1-tert-Butoxypropan-2-ol. Lyon, France: World Health Organization; 2006.
23. de Graaf B, Clore A, McCullough AK. Cellular pathways for DNA repair and damage tolerance of formaldehyde-induced DNA-protein crosslinks. DNA Repair 2009;8:1207–14.
24. Ridpath JR, Nakamura A, Tano K, Luke AM, Sonoda E, Arakawa H, et al. Cells deficient in the FANC/BRCA pathway are hypersensitive to plasma levels of formaldehyde. Cancer Res 2007;67:11117–22.
25. Casanova-Schmitz M, Heck HD. Effects of formaldehyde exposure on the extractability of DNA from proteins in the rat nasal mucosa. Toxicol Appl Pharmacol 1983;70:121–32.
26. Swenberg JA, Barrow CS, Boreiko CJ, Heck HD, Levine RJ, Morgan KT, et al. Non-linear biological responses to formaldehyde and their implications for carcinogenic risk assessment. Carcinogenesis 1983;4:945–52.
27. Casanova M, Morgan KT, Steinhagen WH, Everitt JI, Popp JA, Heck HD. Covalent binding of inhaled formaldehyde to DNA in the respiratory tract of rhesus monkeys: pharmacokinetics, rat-to-monkey interspecies scaling, and extrapolation to man. Fundam Appl Toxicol 1991;17:409–28.
28. Yu R, Lai Y, Hartwell HJ, Moeller BC, Doyle-Eisele M, Kracko D, et al. Formation, accumulation and hydrolysis of endogenous and exogenous formaldehyde induced DNA damage. Toxicol Sci 2015;146:170–82.
29. Lu K, Ye W, Zhou L, Collins LB, Chen X, Gold A, et al. Structural characterization of formaldehyde-induced cross-links between amino acids and deoxynucleosides and their oligomers. J Am Chem Soc 2010;132:3388–99.
30. Swenberg JA, Kerns WD, Mitchell RI, Gralla EJ, Pavkov KL. Induction of squamous cell carcinomas of the rat nasal cavity by inhalation exposure to formaldehyde vapor. Cancer Res 1980;40:3398–402.
31. Kerns WD, Pavkov KL, Donofrio DJ, Gralla EJ, Swenberg JA. Carcinogenicity of formaldehyde in rats and mice after long-term inhalation exposure. Cancer Res 1983;43:4382–92.
32. Monticello TM, Swenberg JA, Gross EA, Leininger JR, Kimbell JS, Seilkop S, et al. Correlation of regional and nonlinear formaldehyde-induced nasal cancer with proliferating populations of cells. Cancer Res 1996;56:1012–22.
33. Zhang L, Steinmaus C, Eastmond DA, Xin XK, Smith MT. Formaldehyde exposure and leukemia: a new meta-analysis and potential mechanisms. Mutat Res 2009;681:150–68.
34. Lu K, Collins LB, Ru H, Bermudez E, Swenberg JA. Distribution of DNA adducts caused by inhaled formaldehyde is consistent with induction of nasal carcinoma but not leukemia. Toxicol Sci 2010;116:441–51.
35. Lehman-McKeeman L. Paracelsus and formaldehyde 2010: the dose to the target organ makes the poison. Toxicol Sci 2010;116:361–63.
36. Beane Freeman LE, Blair A, Lubin JH, Stewart PA, Hayes RB, Hoover RN, et al. Mortality from lymphohematopoietic malignancies among workers in formaldehyde industries: the National Cancer Institute Cohort. J Natl Cancer Inst 2009;101:751–61.
37. Coggon D, Ntani G, Harris EC, Palmer KT. Upper airway cancer, myeloid leukemia, and other cancers in a cohort of British chemical workers exposed to formaldehyde. Am J Epidemiol 2014;179:1301–11.
38. IARC. Formaldehyde, a review of human carcinogens. Part F: chemical agents and related occupations. Lyon, France: World Health Organization; 2012.

39. NTP. 13th Report on Carcinogens. Washington, DC: U.S. Department of Health and Human Services; 2014.
40. ATSDR. Toxicological profile for formaldehyde. Atlanta, GA: U.S. Department of Health and Human Services; 1999.
41. Dhareshwar SS, Stella VJ. Your prodrug releases formaldehyde: should you be concerned? No! J Pharm Sci 2008;97:4184–93.
42. Shi Y, Lan F, Matson C, Mulligan P, Whetstine JR, Cole PA, et al. Histone demethylation mediated by the nuclear amine oxidase homolog LSD1. Cell 2004;119:941–53.
43. Sullivan J, Krieger G. Formaldehyde. Clinical environmental health and toxic exposures. Philadelphia, PA: Lippincott Williams & Wilkins; 2001.
44. Heck HD, Casanova-Schmitz M, Dodd PB, Schachter EN, Witek TJ, Tosun T. Formaldehyde (CH2O) concentrations in the blood of humans and Fischer-344 rats exposed to CH2O under controlled conditions. Am Ind Hyg Assoc J 1985;46:1–3.
45. Casanova M, Heck HD, Everitt JI, Harrington WWJr, Popp JA. Formaldehyde concentrations in the blood of rhesus monkeys after inhalation exposure. Food Chem Toxicol 1988;26:715–6.
46. NTP. Final report on carcinogens background document for formaldehyde. Washington, DC: U.S. Department of Health and Human Services; 2010.
47. Heck HD, White EL, Casanova-Schmitz M. Determination of formaldehyde in biological tissues by gas chromatography/mass spectrometry. Biomed Mass Spectrom 1982;9:347–53.
48. NRC. Review of the environmental protection agency's draft IRIS assessment of formaldehyde. Washington, DC: The National Academies Press; 2011.
49. Shaham J, Bomstein Y, Gurvich R, Rashkovsky M, Kaufman Z. DNA–protein crosslinks and p53 protein expression in relation to occupational exposure to formaldehyde. Occup Environ Med 2003;60:403–9.
50. Ye X, Ji Z, Wei C, McHale CM, Ding S, Thomas R, et al. Inhaled formaldehyde induces DNA-protein crosslinks and oxidative stress in bone marrow and other distant organs of exposed mice. Environ Mol Mutagen 2013;54:705–18.
51. Edrissi B, Taghizadeh K, Moeller BC, Kracko D, Doyle-Eisele M, Swenberg JA, et al. Dosimetry of N(6)-formyllysine adducts following [(1)(3)C(2)H(2)]-formaldehyde exposures in rats. Chem Res Toxicol 2013;26:1421–3.
52. Smith C, Gasparetto M, Humphries K, Pollyea DA, Vasiliou V, Jordan CT. Aldehyde dehydrogenases in acute myeloid leukemia. Ann N Y Acad Sci 2014;1310:58–68.
53. Grafstrom RC, Fornace A Jr, Harris CC. Repair of DNA damage caused by formaldehyde in human cells. Cancer Res 1984;44:4323–7.
54. Casanova M, Morgan KT, Gross EA, Moss OR, Heck HA. DNA-protein crosslinks and cell replication at specific sites in the nose of F344 rats exposed subchronically to formaldehyde. Fundam Appl Toxicol 1994;23:525–36.
55. Stingele J, Habermann B, Jentsch S. DNA-protein crosslink repair: proteases as DNA repair enzymes. Trends Biochem Sci 2015;40:67–71.